LIQUEFACTION SUSCEPTIBILITY MAPPING OF THE SHALLOW ALLUVIUM, INNER VALLEY, RIO GRANDE BASIN, ALBUQUERQUE, NEW MEXICO

By

Jodi A. Clark

Submitted in Partial Fulfillment
of the Requirements for the Degree of
Master of Science in Geology

New Mexico Institute of Mining and Technology
Department of Earth and Environmental Science

Socorro, New Mexico

May, 2004

In memory of

Ms. Shirley Shook

and

Mr. Stanley Corne

ABSTRACT

Albuquerque lies within the seismically active Albuquerque Basin, one of the largest tectonic basins within the Rio Grande rift. Although there have been few large historical earthquakes, there are many Quaternary faults in the Albuquerque area. Therefore, there is a potential for future earthquakes and liquefaction related damage in the region. The purpose of this study is three-fold: 1) To develop a database of shallow geotechnical borehole data for use in this study and for the benefit of future work in this study area, 2) To establish three-dimensional GIS-based procedures for evaluating liquefaction susceptibility, and 3) To compare the results of these methods to an existing two-dimensional liquefaction susceptibility study for the same area.

The study area for this project is restricted to the Inner Valley of the Albuquerque Basin and extends from the southern boundary of Sandia Pueblo to the northern boundary of Isleta Pueblo. The Inner Valley is a 4.5 to 6.5 km (2.8 to 4 mi) wide lowland valley and floodplain that is underlain by unlithified and predominantly sandy alluvium. Clay and gravel lenses are locally present but generally not laterally persistent. The shallow water table in this region intersects the ground surface along the Rio Grande and gently slopes away from the river in both directions.

The first phase of this study was to compile a database of well log information for use in engineering geologic and liquefaction susceptibility studies. Data from 407 boreholes were included in this database. This database was the basis for study of the

spatial distribution of shallow alluvial sediments within the Inner Valley of the Albuquerque Basin and GIS-based liquefaction susceptibility analyses.

A recent liquefaction susceptibility study of the Albuquerque area focused on the surficial geology and did not take into account vertical variations of soils that could cause potential liquefaction problems. I developed a GIS-based approach to incorporate these vertical variations by evaluating liquefaction susceptibility for three depth intervals and then combining these to form the overall liquefaction susceptibility for the study area. I also developed a second GIS-based method that used standardized standard penetration test (SPT) blow count data as a proxy for the calculated peak ground acceleration (PGA) trigger to minimize data calculation and processing time. The data for this study are clustered, sparse, and show a high level of spatial variability. These characteristics create some uncertainty with the GIS based liquefaction susceptibility analysis on a regional scale, but would likely not pose a problem with more localized analyses with more evenly distributed data.

The results of these two methods are compared to the previous surficial geology based results. The three methods can be compared, but there is no way to evaluate the relative or absolute accuracy of the three methods for liquefaction susceptibility presented in this study and be able to definitively say any one is better than another unless they are compared to the resultant liquefaction in the event of an earthquake. All three methods show the same regional trend, which is highest risk of liquefaction along the river and floodplain with decreasing liquefaction susceptibility to the east and west as the elevation increases and the depth to groundwater increases. Each of the methods is best suited to particular uses, but none of them are without uncertainty or inherent error.

The surficial geology approach used in the previous study provides a regional overview of the liquefaction susceptibility distribution, but masks some localized areas were the potential for liquefaction could be higher than the surficial geology indicates, and should primarily be applied to areas with little or no vertical variability. The methods developed for this study provide more localized detail, but when applied on a regional scale introduce uncertainty and bias based on the distribution of the data.

ACKNOWLEDGEMENTS

I would like to begin by thanking Dr. Bill Haneberg and Dr. Laurel Goodwin, my advisers on this project, for their encouragement and support. Laurel I would have never made it if not for your patience, guidance, and faith in my abilities. I would also like to thank Dr. Peter Mozley and Dr. Harold Tobin for serving on my committee.

This project would not have been possible with out the initial financial support of the State of New Mexico Department of Public Safety Emergency Preparedness Division and the New Mexico Bureau of Geology and Mineral Resources. I would also like to thank Keith Kelson and Chris Hitchcock of William Lettis & Associates for their help and data sharing over the course of this project. I would also like to thank the numerous people at the following organizations that provided the much needed data that made this study possible: the New Mexico Environment Department, the New Mexico State Highway and Transportation Department, the City of Albuquerque, and the United States Geological Survey.

In addition, I would like to thank Mark Mansell, Glen Jones, Sean Connell, Dr. Dave Love, Dr. Bruce Allen, and Dr. John Hawley of the New Mexico Bureau of Geology and Mineral Resources for all of their advice and support throughout the many twists and turns of this project. An extra special thanks to Mark Mansell for allowing me loads of disk space and work time on his computer over the last several years and for helping me figure out ways to accomplish some of the GIS tasks.

I also thank Dr. Geoff Rawling and Sunny Baer for acting as peer reviewers and just for being there with their support, advice and encouragement.

I must also thank everyone at Hydrosphere for their support and encouragement; for giving me the opportunity of full time work in my field, for not giving up on me, and for giving me the flexibility I needed to finish up my thesis and work at the same time.

I would also like to thank all my family and friends, Robert and Betty Sigmon, Suzi Brown, John Clark, Lois Thompson, Dr. Loren Raymond, Pat Mills, Elizabeth Crane, Sharon Fulligim, Skeeter Leard, and Margi Lucena for the unconditional love and support they provided and having faith in me over the years. Thanks also to all the members of LES for providing much needed down time and diversions and for your support and encouragement.

I would especially like to acknowledge my appreciation for the years of love, support and encouragement provided by Natasha Isenhour. I couldn't have done it without you. Thanks so much for keeping the faith.

TABLE OF CONTENTS

LIST OF TABLES

LIST OF FIGURES

CHAPTER 1. INTRODUCTION

1.1 Statement of the Problem

Liquefaction has been defined as the transformation of a granular material from a solid state into a liquefied state as a consequence of increased pore-water pressures (Youd, 1973,1975; Youd and Hoose, 1978). Liquefaction can cause major property damage as well as loss of life. The Inner Valley of the Rio Grande River near Albuquerque, New Mexico is a prime location for potential liquefaction in the event of a major earthquake. All the necessary ingredients for disaster are there: a geologic history of seismic activity; widely distributed saturated and predominately sandy deposits at shallow depths; and a large urban center. Therefore, it is useful to delineate areas that are most susceptible to liquefaction. Liquefaction susceptibility maps can be used to identify areas of potentially liquefiable sediments where caution should be exercised when new facilities are being designed or existing facilities renovated (Power and Holzer, 1996).

1.2 Scientific and Societal Significance

Seismically generated ground failure including landslides, lateral spreads, ground cracks, and differential settlement have been the cause of much of the historic earthquake damage and casualties (Youd and Hoose, 1978). In many cases these ground failures are caused by liquefaction. Liquefaction occurs when saturated, sandy soils that are not cohesive (e.g. because clays are absent) are subjected to intense shaking. The soil loses

its strength and undergoes a transition from a solid state to a dense flowing liquid state because of increased pore-water pressure. The increase in pore water pressure occurs when a shear wave caused by earthquake shaking passes through saturated granular soils causing the collapse of the granular structure and a decrease in pore space. This decrease in pore space in turn causes an increase in pore water pressure. If the pore water pressure increases to the point where the soil's shear strength can no longer support the overlying weight then the soil loses cohesion and begins to flow as a liquid.

Historical accounts of the New Madrid (Missouri) earthquakes in 1811 and 1812 describe high banks caving into the Mississippi River, sandbars giving way and disappearing, and large areas covered with water that emerged from below the ground through fissures (Bolt, 1993). In total, raised and sunken lands, sandblows, soil sinks, fissures, and large landslides affected an area of over 90,000 square kilometers.

The 1906 San Francisco (California) earthquake caused ground failures over a 370 mile (600 km) long segment of the Coast Ranges of California (EQE, 1989). Liquefaction and settlement caused damage to water mains and wharfs in Oakland and extensive damage in the South Market area of San Francisco.

The 1989 Loma Prieta (California) earthquake caused liquefaction damage in a very similar pattern to what occurred in 1906 in San Francisco (EQE, 1989). Thousands of landslides occurred causing damage to residential developments and roads. The damage estimates from direct damage and business interruption were approximately $10 billion while direct damage alone was $6.8 billion. More than 62 people died and over 3,700 were reported injured. At least 12,000 people were displaced with the damage to

more than 18,000 homes. Close to 1,000 homes and 150 buildings were destroyed, and another 2,500 buildings were damaged.

The 1995 Kobe earthquake in Japan caused extensive liquefaction related ground failures, which affected buildings, highways, the port, and underground infrastructure, and hampered recovery efforts (EQE, 1995). The areas most affected were located primarily along the coastline and waterways in the Kobe and Osaka vicinity, where the soils are primarily soft alluvium and artificial fills. Settlement and liquefaction of less than 50 cm to as much as 3 m were observed. Underground utilities, including gas, water, and sewer lines, were severely damaged and large parts of the mainland and the reclaimed islands were without these services for close to a month. The total direct damage for this earthquake was estimated at $147 billion dollars and does not include indirect economic effects from business interruption and loss of life. Approximately 5,500 people were killed, 35,000 were injured, and more than 300,000 were left homeless the night of the earthquake. 180,000 buildings were badly damaged or destroyed.

The 1964 earthquakes in Alaska, United States and Niigata, Japan also caused significant damage due to liquefaction related ground failures and marked the beginnings of studies to understand and mitigate liquefaction hazard (NCEER, 1997; Youd, 1999). Following these earthquakes, Seed and Idriss (1971) developed and published the initial Seed Simplified Procedure (SSP), which has continued to evolve over the last thirty years as the standard procedure for evaluating the liquefaction resistance of soils throughout North America and much of the world. The SSP was developed on the basis of field and laboratory test data, and it has been improved as additional data has become available and more studies have been completed. Use of the SSP requires the calculation or estimation

of two variables: the seismic demand placed on a soil layer expressed as the cyclic stress ratio (CSR) and the capacity of the soil to resist liquefaction expressed as the cyclic resistance ratio (CRR). The term "soil" as used in this study refers to the engineering definition, such that soils are all unlithified materials above the bedrock.

1.3 Generalized Project Approach

The purpose of this study was three-fold: 1) To develop a database of shallow geotechnical borehole data for use in this study and for the benefit of future work in this study area, 2) To establish three-dimensional GIS-based procedures for evaluating liquefaction susceptibility based on the SSP, 3) To compare the results of these methods to an existing and primarily two-dimensional liquefaction susceptibility study for the same area.

Developing methods of determining liquefaction potential has been the focus of many studies (Seed *et al.,* 1983, 1985, 1986; Poulos *et al.,* 1985). Other studies have proposed using a Geographic Information System (GIS) in liquefaction risk analyses (Luna, 1993; Macari *et al.,* 1993; Martin, 1993; Ostadan *et al.,* 1993; Real, 1993). GIS can provide a means of organizing, analyzing, and presenting the data necessary for creating a liquefaction susceptibility map very easily and efficiently, especially now that desktop versions are widely available.

This study incorporates the Seed Simplified Procedure (SSP) and a GIS-based approach. The evaluation of the liquefaction susceptibility of the soils is based on the calculations and the guidelines set out by the SSP, and the GIS is used to facilitate

management of the data, interpolation of the data over the study area, and presentation of the results. The following chapter provides detailed background on the geologic setting of the study area, the underlying SSP methods, and an explanation of the 2-D liquefaction susceptibility study used as a comparison to the current study in order to lay the foundation for the development of the 3-D method used in the current study.

CHAPTER 2. PREVIOUS WORK

2.1 Geologic Setting

Albuquerque lies within the seismically active Albuquerque Basin, one of the largest tectonic basins within the Rio Grande rift. Although there have been few large historical earthquakes, there are many Quaternary faults in the area. The study area for this project is restricted to the Inner Valley of the Albuquerque Basin and extends from the southern boundary of Sandia Pueblo to the northern boundary of Isleta Pueblo. Figure 1 shows the study area boundary superimposed on a shaded digital elevation model that emphasizes the inner valley and the abrupt changes in elevation that mark the eastern and western boundaries. The Inner Valley is a 4.5 to 6.5 km wide lowland valley and floodplain that is underlain by unlithified, uncemented, and predominantly sandy alluvium. Clay and gravel lenses are locally present but generally not laterally persistent. The shallow water table in this region intersects the ground surface along the Rio Grande and gently slopes away from the river in both directions (Thorn *et al.,* 1993).

The Albuquerque Basin is located in central New Mexico and covers approximately 7,800 sq km (Figure 2). It extends from the San Felipe fault belt near Algodones south to the Joyita uplift at the north end of the Socorro structural basin (Kelley, 1977; Hawley, Haase and Lozinsky, 1995). It is one of the largest in series of north-trending structural basins that comprise the Rio Grande rift. The basin is approximately 110 km long and varies from 16-65 km wide. It is bounded on the east by

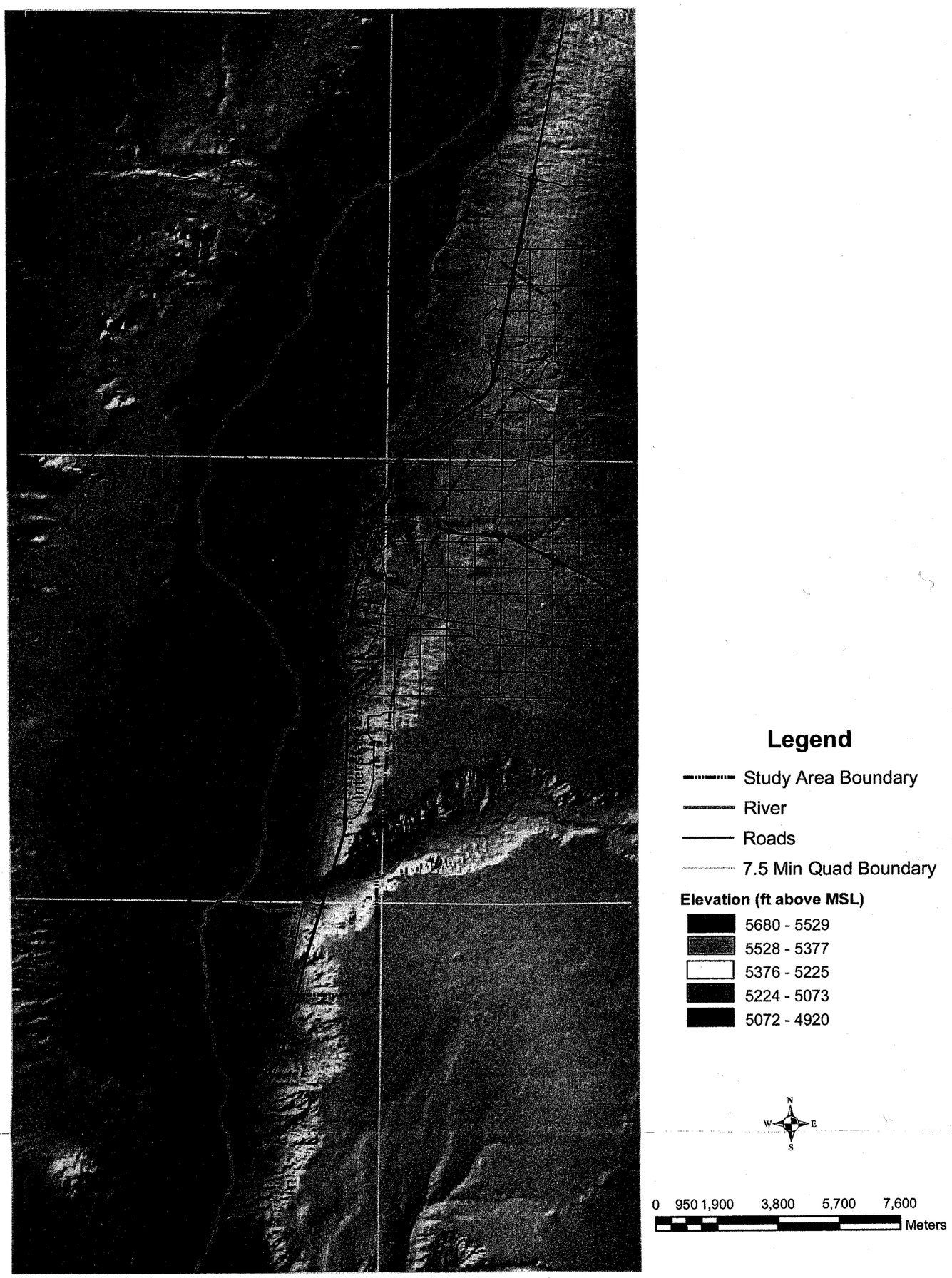

Figure 1. Map Showing location of study area.

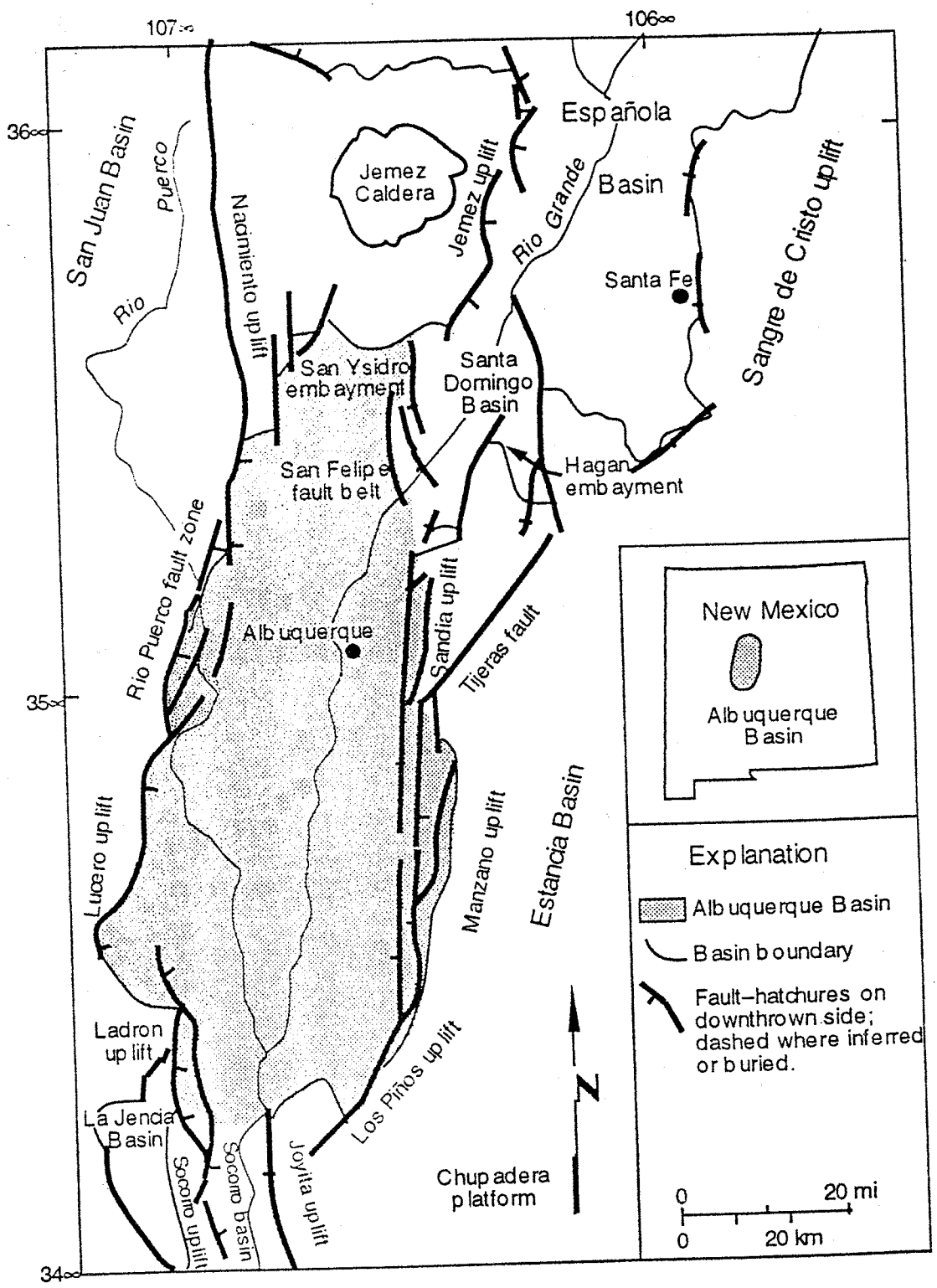

Figure 2. Index map of the Albuquerque Basin showing location of major boundary faults and features (modified from Hawley and Haase, 1992).

the Sandia-Manzano-Los Pinos uplift. The western boundary with the Colorado Plateau is not prominently defined. The southwestern boundary is defined by the Ladron Mountains and Lucero uplift.

Deposits in the Albuquerque Basin are composed primarily of three units: 1) pre-Santa Fe Group Tertiary deposits, 2) Santa Fe Group basin fill, and 3) post-Santa Fe Group Quaternary deposits (Hawley and Haase, 1992). This study focuses primarily on soils that are within the post-Santa Fe Quaternary deposits, specifically the Valley Fill facies subdivision of hydrostratigraphic units River Alluvium (RA), River-Terrace Alluvium (TA) and Arroyo-Valley Alluvium (VA) as designated by Hawley and Haase (1992). More recent mapping and differentiation of these post-Santa Fe Group deposits has been done by Connell and others and is ongoing (Connell, 1997, 2001; Connell *et al.*, 1998; Connell and Love, 2001). These post-Santa Fe Quaternary deposits are the result of a series of river incision and partial backfilling episodes (Hawley and Haase, 1992; Hawley, Haase and Lozinsky, 1995; Hawley and Whitworth, 1996). The present Inner Valley channel and floodplain deposits are a result of the latest cut-and-fill episode within the Rio Grande – Rio Puerco system. These youngest valley fill deposits are the result of ten to fifteen thousand years of aggradation and form the shallow aquifer, which can be up to 40 meters thick. These units are dominantly sand and gravel channel deposits with localized silt and clay rich overbank deposits.

The most seismically active region in New Mexico is the area within the Rio Grande rift between Albuquerque and Socorro, according to historic and instrumental records since 1849 (Sanford *et al.*, 1981). Only 6 earthquakes occurring in the Rio Grande rift during this time period have had an estimated Richter magnitude (M_L) of 5.0

or greater (Modified Mercalli (MM) VI; Wong *et al.,* 2000). However, the paleosiesmic record throughout the rift indicates large prehistoric earthquakes (M > 6) with surface ruptures have occurred. There are well over one hundred Quaternary faults in the rift, and at least 20 of them show evidence for movement during the Holocene (last 10,000 yrs; Hawley and Whitworth, 1996; Machette, 1998; Machette *et al.,* 1998; Personius, Machette and Kelson, 1999). The locations of Quaternary faults in the Albuquerque area are shown in Figure 3 and are indexed in Table 1. Because of this potential, the Uniform Building Code (1994) considers Albuquerque to lie within zone 2B, indicating a moderate seismic hazard (Figure 4).

Recent work by Wong and others (2000) resulted in nine hazard microzonation maps for the Albuquerque-Belen-Santa Fe corridor, including earthquake scenario maps based on an M_w 7.0 earthquake along the Sandia-Rincon fault just east of Albuquerque and probabilistic maps for 10% and 2% probability of exceedance in 50 years. It is important to note that "although large earthquakes may be infrequent on a specific fault the large number of faults in the corridor indicate that the probability of a large earthquake occurring somewhere in the corridor is not insignificant" (Wong *et al.,* 2000).

A summary of detailed studies of seismicity in the Rio Grande rift of New Mexico by Sanford and others (1991) show that seismicity since 1961 has been diffuse and only locally associated with specific tectonic or structural features. Detailed studies of the Albuquerque area show that seismicity is limited to the upper 12 to 13 km of crust. Focal mechanisms indicate both strike-slip and normal faulting and an orientation of minimum principal stress approximately WNW-ESE (Sanford *et al.,* 1991).

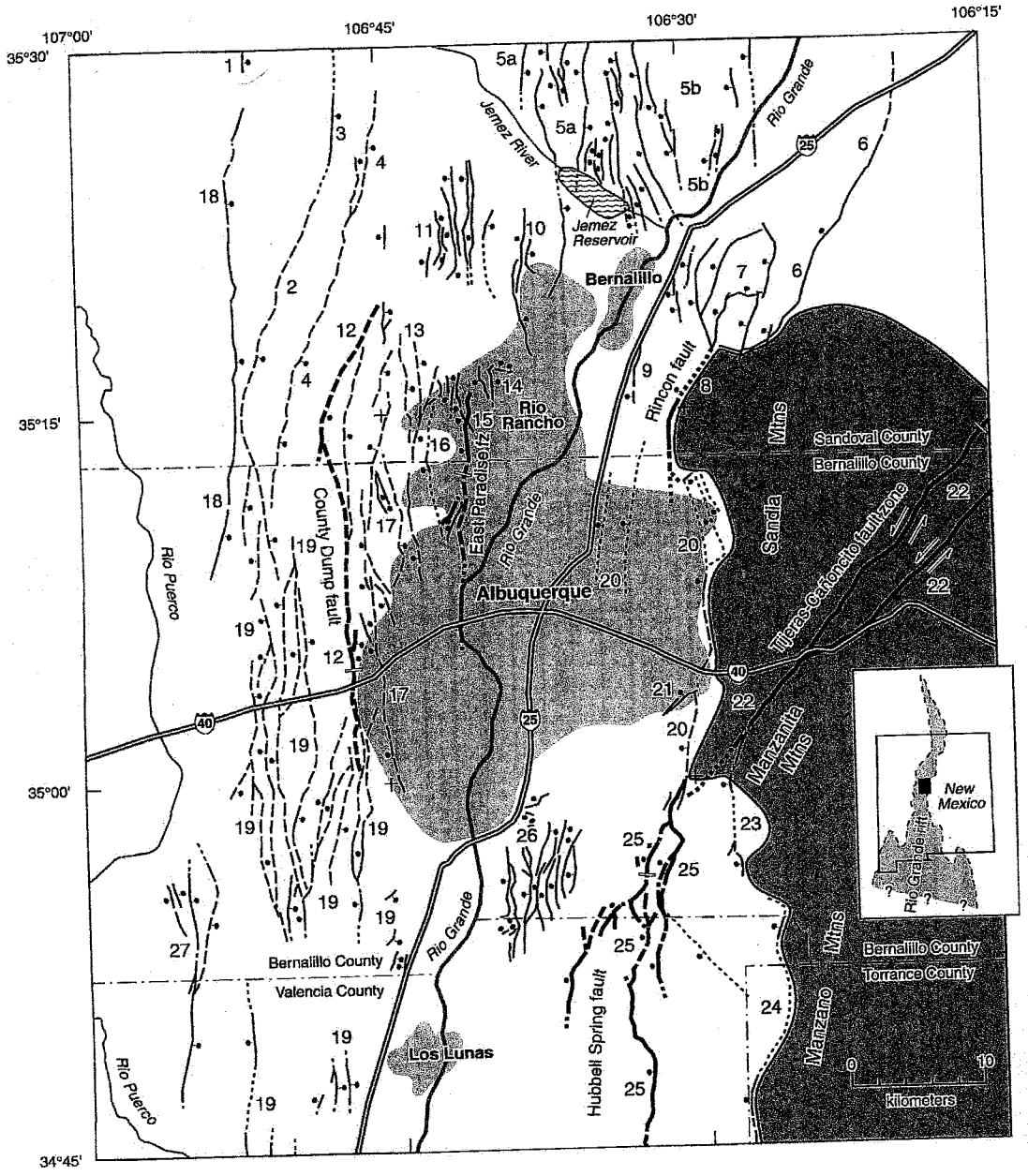

Figure 3. Map showing locations of Quaternary faults near Albuquerque, New Mexico. Lightly shaded area shows urbanized areas. Shaded and stippled area represents pre-Tertiary rocks in the Sandia, Manzanita, and Manzano Mountains (from Personius, Machette, and Kelson, 1999). Key to faults is in Table 1.

Table 1. Quaternary fault data key to Figure 3 (from Personius *et al.*, 1999)

Fault Number	Number in Database[1]	Name of Fault	MRE[2]	Length[3] (km)	Fault type, dip direction
1	2002b	Nacimiento fault, southern section	<750 ka	45	Reverse, normal, E & W
2	2035	Calabacillas fault	<750 ka	40	Normal, E
3	2029b	Jemez-San Ysidro fault, San Ysidro section	<750 ka	34	Normal, E
4	2046	Zia fault	<750 ka	32	Normal, E
5a	2030a	San Felipe fault, Santa Ana section	<1.6 Ma	NA	Normal, E
5b	2030b	San Felipe fault, Algodones section	<1.6 Ma	NA	Normal, W
6	2031	San Francisco fault	<1.6 Ma	26	Normal, W
7	2043	Faults north of Placitas	<750 ka	NA	Normal, NW
8	2036	Rincon Fault	<15 ka	12	Normal, W
9	2034	Bernalillo fault	<750 ka	6	Normal, W
10	2045	Unnamed faults near Loma Barbon	<1.6 Ma	NA	Normal, W & E
11	2041	Unnamed faults near Picuda Peak	<1.6 Ma	NA	Normal, E & W
12	2038	County Dump fault	<130 ka	35	Normal, E
13	2048	Unnamed faults near Star Heights	<750 ka	NA	Normal, E>W
14	2047	Unnamed faults near Loma Colorado de Abajo	<1.6 Ma	NA	Normal W, & Normal (?) N
15	2040	East Paradise fault zone	<130 ka	>13	Normal, W
16	2042	West Paradise fault zone	<750 ka	10	Normal, W
17	2049	Unnamed faults near Albuquerque Volcanoes	<750 ka	NA	Normal, E & W
18	2039	Sand Hill fault zone	<1.6 Ma	36	Normal, E
19	2121	Faults on Llano de Albuquerque	<750 ka	NA	Normal, E & W
20	2037	Sandia fault	<750 ka	NA	Normal, W
21	2044	Four Hills Ranch fault	<750 ka	3	Normal (?), NW (?)
22	2033b	Tijeras-Cañoncito fault system, Canyon section	<130 ka	42	Sinistral, vertical
23	2128	Coyote fault	<750 ka	11	Normal, W
24	2119	Manzano fault	<750 ka	54	Normal, W
25	2120	Hubbell Spring fault	<130 ka	NA	Normal, W
26	2135	McCormick Ranch fault	<750 ka	NA	Normal, E & W
27	2122	Cat Mesa fault	<750 ka	20	Normal, E

[1] Fault number from Machette *et al*. (1998)

[2] Most recent surface-faulting event, age in ka (thousands of years); categories from Machette *et al*. (1998)

[3] Rounded length from Machette et al. (1998); NA - not applicable for groups of individual faults or complex fault zones

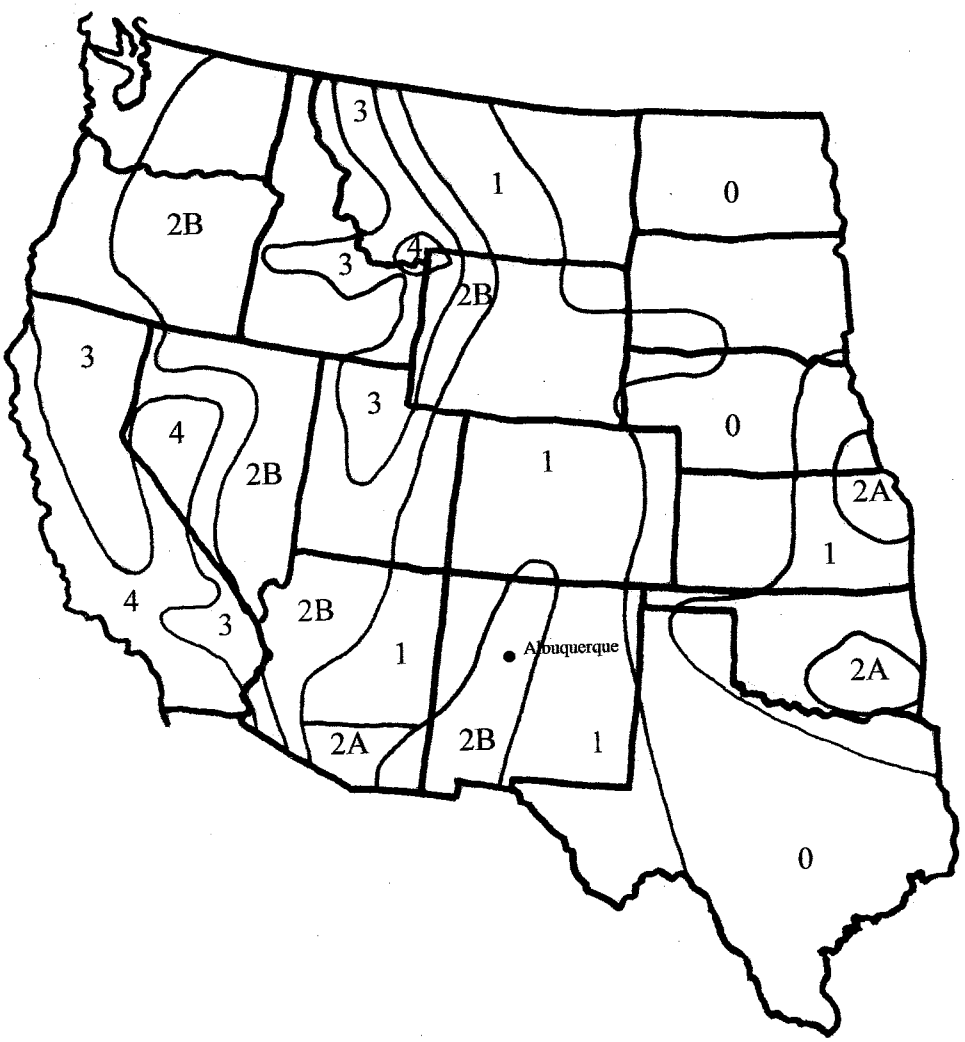

Figure 4. 1994 Uniform Building Code seismic zone map. Zone 0 = Very low hazard, Zone 1 = Low hazard, Zone 2A, 2B = Moderate hazard, Zone 3 = High hazard, and Zone 4 = Extreme hazard.

2.2 Liquefaction Susceptibility Analysis Background

Liquefaction susceptibility maps indicate the qualitative or quantitative ranking (low, medium, and high) of susceptibility of soils/sediments to liquefaction. A variety of geologic and engineering criteria can be used to assess liquefaction susceptibility, including surficial geology, evidence of historic liquefaction, depth to groundwater, soil boring data, standard penetration test (SPT) blow count analyses, and cone penetration test (CPT) resistances (Power and Holzer, 1996). All methods discussed in this paper are based on the Seed Simplified Procedure (SSP) and subsequent revisions (Seed and Idriss, 1971, 1982; Seed, 1979; Seed *et al.,* 1983, 1985; NRC, 1985; Seed and Harder, 1990; NCEER, 1997; Idriss, 1997; Robertson and Wride, 1997; Youd, 1997). The SSP has evolved over the last thirty years as the standard procedure for evaluating the liquefaction resistance of soils throughout North America and much of the world. In 1985 and 1996, workshops were convened to review and update the SSP for assessing liquefaction hazard and evaluating liquefaction resistance. The SSP was developed on the basis of field observations and field and laboratory test data. The SSP provides a verified method for evaluating liquefaction hazard where sites are primarily "level to gently sloping terrain underlain by Holocene alluvial or fluvial sediment at shallow depths (less than 15 m (50 ft))" (NCEER,1997). Use of the SSP requires the calculation or estimation of two variables: the seismic demand placed on a soil layer expressed as the cyclic stress ratio (CSR) and the capacity of the soil to resist liquefaction expressed as the cyclic resistance ratio (CRR; NCEER, 1997).

The following largely empirical formula, developed by Seed and Idriss (1971), is used to estimate CSR:

$$CSR = 0.65\left(\frac{a_{\max}}{g}\right)\left(\frac{\sigma_{vo}}{\sigma'_{vo}}\right)r_d \qquad (1)$$

where a_{max} is the peak horizontal acceleration at ground surface generated by the earthquake, g is the acceleration due to gravity, σ_{vo} is the total vertical overburden stress, σ'_{vo} is the effective vertical overburden stress, and r_d is a stress reduction coefficient. The CSR value could also be obtained in the laboratory through cyclic testing of undisturbed soil samples, but this is an expensive and difficult process, and empirical correction factors are still needed to relate the laboratory values to field approximations. The stress reduction coefficient provides an approximate correction for the flexibility of the soil profile, and can be estimated by the following equations:

$$r_d = 1.0 - 0.00765z \qquad \text{for } z \leq 9.15 \text{ m} \qquad (2a)$$

$$r_d = 1.174 - 0.0267z \qquad \text{for } 9.15 < z \leq 23 \text{ m} \qquad (2b)$$

$$r_d = 0.744 - 0.008z \qquad \text{for } 23 < z \leq 30 \text{ m} \qquad (2c)$$

$$r_d = 0.50 \qquad \text{for } z > 30 \text{ m} \qquad (2d)$$

where z is the depth below ground surface in meters. Liao and Whitman (1986) proposed equations 2a and 2b, equation 2c was added by Robertson and Wride (NCEER, 1997), and equation 2d was contributed by Marcuson in post-workshop dialog (NCEER, 1997). Figure 5 shows a plot of r_d versus depth. It is important to note that using mean values of r_d increases uncertainty in the calculation of CSR with depth, and that the SSP is not verified for depths greater than 15m (50 ft; NCEER, 1997).

Evaluating the liquefaction resistance component, CRR, is more of a challenge. Collecting and analyzing undisturbed samples using laboratory cyclic testing of seismic

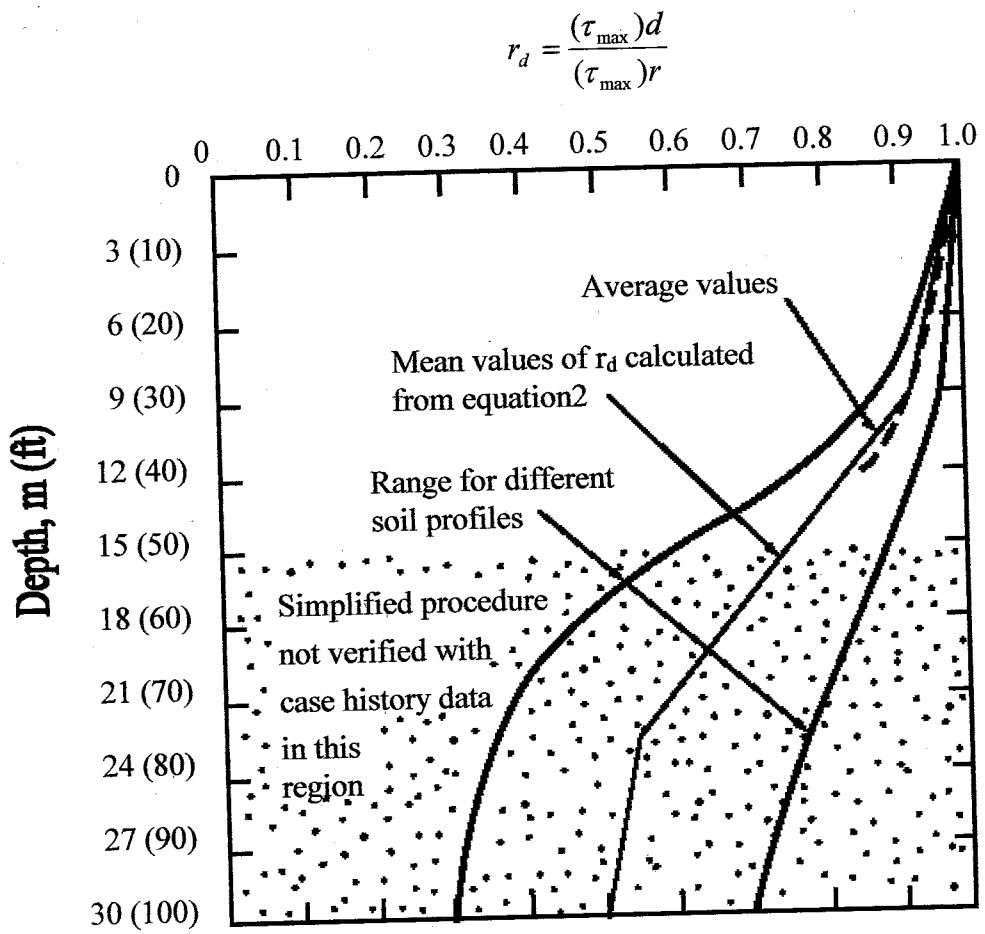

Figure 5. Plot of r_d versus depth curves developed by Seed and Idriss (1971) with added mean value lines from Equation 2 (from NCEER, 1997).

loading is prohibitively costly; therefore, standard field tests such as the standard penetration test (SPT), the cone penetration test (CPT), and shear wave velocity measurements (V_s) have become routine for liquefaction resistance evaluations (NCEER, 1997). Evaluation of liquefaction resistance based on SPT blow counts has been well established and the criteria refined over the years. Figure 6 is a plot of CSR versus normalized SPT N-value $(N_1)_{60}$ for locations throughout the world where liquefaction was and was not observed after earthquakes. Also included on this plot are CRR curves for magnitude 7.5 earthquakes separating data representative of liquefaction susceptible sediments from those representative of liquefaction resistant sediments. The SSP basic penetration criterion is the CRR curve for fines content less than or equal to five percent (Figure 6). This curve has been defined as the "simplified base curve." SPT results can be affected by many factors such as fines content, soil plasticity, overburden pressure, energy ratio, borehole diameter, rod length, and sampling method. Table 2 summarizes correction factors for updating SPT measured penetration resistance values (N_M) to the normalized N-value ($(N_1)_{60}$) using the following equation:

$$(N_1)_{60} = N_M C_N C_E C_B C_R C_S \qquad (3)$$

where N_M is the measured SPT resistance, C_N is the correction factor for overburden pressure, C_E is the correction factor for hammer energy ratio, C_B is the correction factor for borehole diameter, C_R is the correction factor for rod length, and C_S is the correction factor for samplers with or without liners. It is also necessary to correct for fines content. The NCEER workshop (1997) recommended procedure for correcting SPT resistance for silty sands to an equivalent clean sand penetration resistance is to use the following equation:

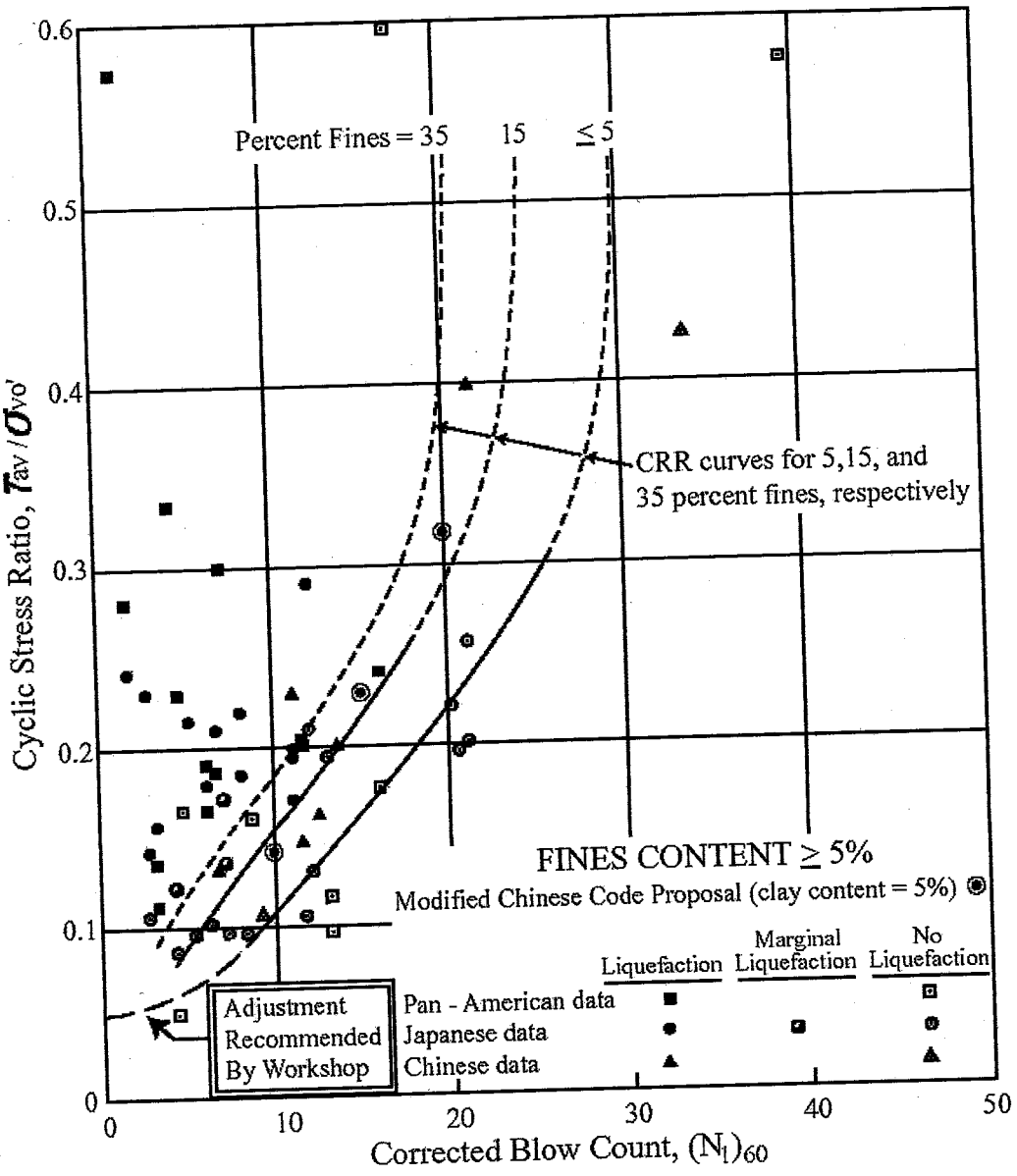

Figure 6. Plot of Corrected Blow Count ($(N_1)_{60}$) versus Cyclic Stress Ratio (CSR) showing the simplified base curve for calculation of Cyclic Resistance Ratio (CRR) from SPT Data along with empirical liquefaction data (modified from NCEER, 1997).

Table 2. Corrections to SPT (from NCEER, 1997).

Factor	Equipment Variable	Term	Correction
Overburden Pressure		C_N	$(P_a/\sigma'_{vo})^{0.5}$
			$C_N \leq 2$
Energy Ratio	Donut Hammer	C_E	0.5 to 1.0
	Safety Hammer		0.7 to 1.2
	Automatic-Trip Donut-		0.8 to 1.3
	Type Hammer		
Borehole Diameter	65 mm to 115 mm	C_B	1
	150 mm		1.05
	200 mm		1.15
Rod Length	3 m to 4 m	C_R	0.75
	4 m to 6 m		0.85
	6 m to 10 m		0.95
	10 m to 30 m		1
	> 30 m		<1.0
Sampling Method	Standard sampler	C_S	1
	Sampler without liners		1.1 to 1.3

$$(N_1)_{60cs} = \alpha + \beta(N_1)_{60} \quad (4)$$

where α and β are empirical coefficients calculated using the following equations:

$$\alpha = 0 \quad \text{for } FC \leq 5\% \quad (5a)$$

$$\alpha = \exp[1.76 - (190/FC^2)] \quad \text{for } 5\% < FC < 35\% \quad (5b)$$

$$\alpha = 5.0 \quad \text{for } FC \geq 35\% \quad (5c)$$

$$\beta = 1.0 \quad \text{for } FC \leq 5\% \quad (6a)$$

$$\beta = [0.99 + (FC^{1.5}/1000)] \quad \text{for } 5\% < FC < 35\% \quad (6b)$$

$$\beta = 1.2 \quad \text{for } FC \geq 35\% \quad (6c)$$

where FC is laboratory measured fines content. The CRR must also be corrected for earthquake magnitudes other than 7.5. This can be accomplished by using a magnitude scaling factor (MSF). Table 3 gives a range of magnitude scaling factors defined by various researchers. The NCEER workshop participants suggest that for magnitudes greater than 7.5 the factors recommended by Idriss should be used. For magnitudes less than 7.5 the engineer or geologist should choose from a range of values depending on the conservatism required for the project, with the values recommended by Idriss defining the lower bound and the values proposed by Andrus and Stokoe (2000) the upper bound of the range. The simplified base curve can be approximated by the following empirical equation for $(N_1)_{60}$ less than 30 and greater than 3:

$$CRR_{7.5} = \frac{a + cx + ex^2 + gx^3}{1 + bx + dx^2 + fx^3 + hx^4} \quad (7)$$

Table 3. Magnitude scaling factor values defined by various investigators.

Magnitude (M)	Seed and Idriss (1982)	Idriss (from Youd and Noble, 1997)	Ambraseys (1988)	Arango (1996)		Andrus and Stokoe (2000)	Youd and Noble (1997)		
							P_L<20%	P_L<32%	P_L<50%
5.5	1.43	2.20	2.86	3.00	2.20	2.80	2.86	3.42	4.44
6.0	1.32	1.76	2.20	2.00	1.65	2.10	1.93	2.35	2.92
6.5	1.19	1.44	1.69	1.60	1.40	1.60	1.34	1.66	1.99
7.0	1.08	1.19	1.30	1.25	1.10	1.25	1.00	1.20	1.39
7.5	1.00	1.00	1.00	1.00	1.00	1.00			1.00
8.0	0.94	0.84	0.67	0.75	0.85	0.8?			0.73?
8.5	0.89	0.72	0.44			0.65?			0.56?

where $x = (N_1)_{60}$; $a = 0.048$; $b = -0.1248$; $c = -0.004721$; $d = 0.009578$; $e = 0.0006136$; $f = -0.0003285$; $g = -1.673E-05$; and $h = 3.714E-06$ (NCEER, 1997).

2.3 WLA Method of Liquefaction Susceptibility

Under the United States Geological Survey National Earthquake Hazards Reduction Program (USGS NEHRP) Award Number 98-HQ-GR-1009, William Lettis & Associates, Inc. (WLA) evaluated liquefaction susceptibility in the Inner Rio Grande Valley near Albuquerque, New Mexico. This area includes and extends to the north and south of the study area for the current project (Figure 7). The database I developed for and included in the current study were used by WLA. Additional data compiled by WLA were also included in the database. The method used by WLA involved four steps illustrated by Figure 8: 1) creation of maps of the surficial geology, 2) creation of maps of depth to water, 3) evaluation of liquefaction susceptibility of near surface soils based on geotechnical borehole data, and 4) creation of a liquefaction susceptibility map based on the data from previous steps (Kelson *et al.*, 1999).

Kelson *et al.* (1999) include a detailed discussion of the procedure used in each of the above steps. A brief overview is provided here to facilitate a comparison of the WLA method and results with other liquefaction susceptibility analyses presented herein.

Surficial Geologic Mapping

The first step in the WLA approach to analysis of liquefaction susceptibility was the mapping of upper Quaternary deposits. The delineation of these deposits was based

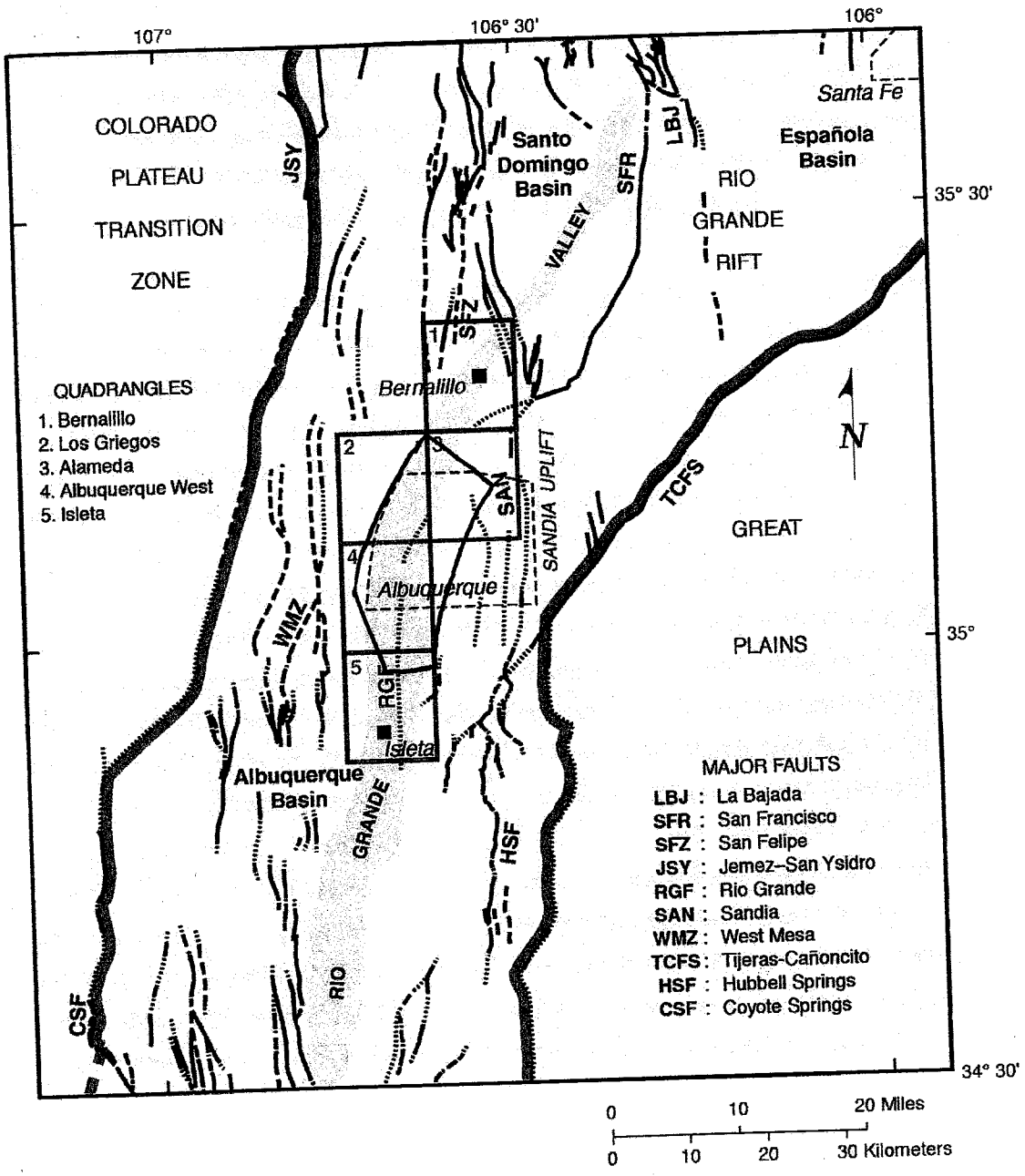

Figure 7. Map showing location of WLA study area (within green quad boundary) and JAC study area for comparison (solid blue line; modified from Kelson *et al.*, 1999).

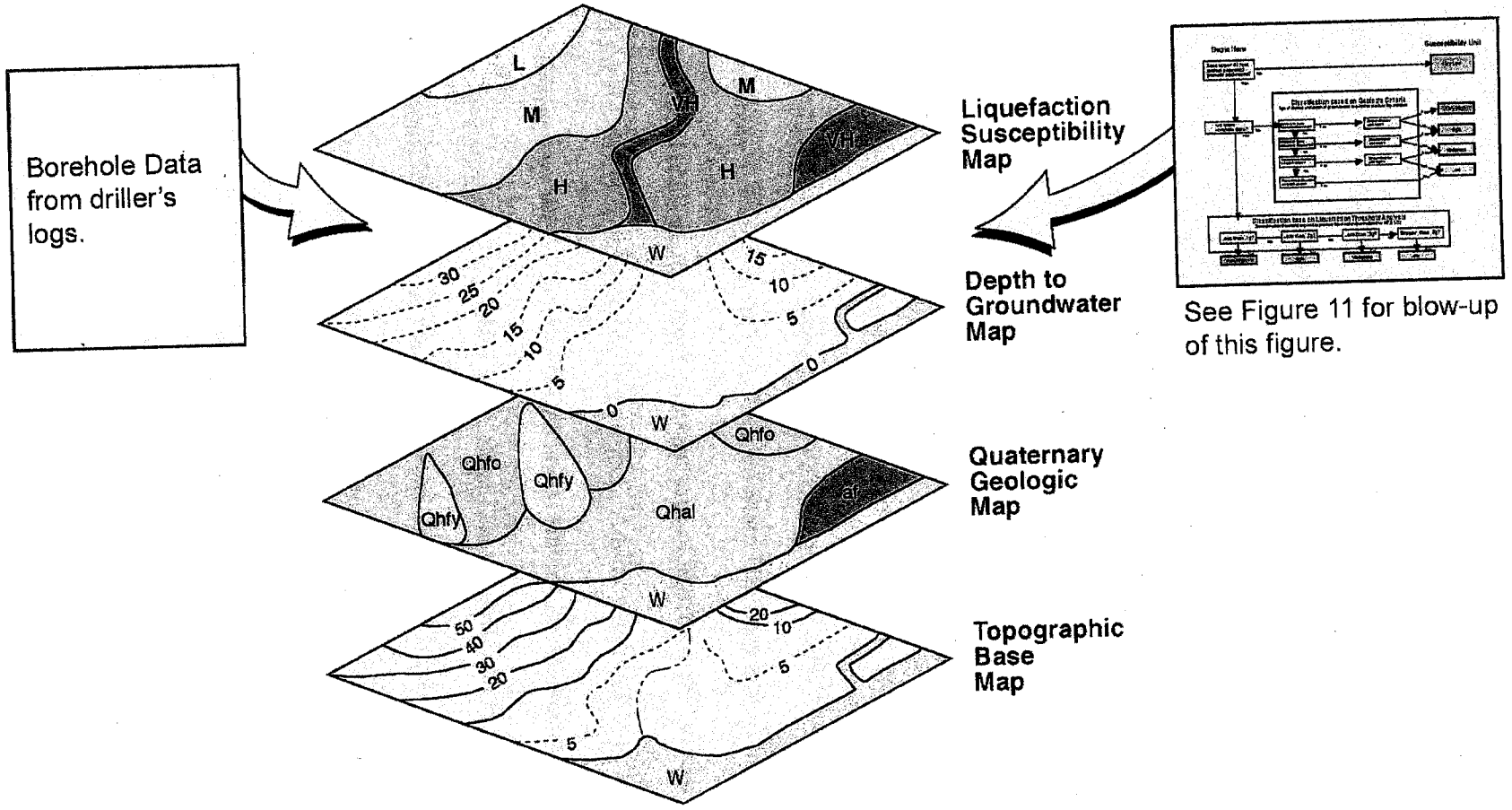

Figure 8. WLA components and procedures for developing a liquefaction susceptibility map (modified from Kelson *et al.*, 1999).

on aerial photography, field reconnaissance, and compilation of data provided by existing geologic maps, soil surveys, and topographic maps (Kelson *et al.,* 1999). Historical flooding information was also collected to help define the extent of historical floodplain deposits. Figure 9 shows the surficial geologic map used in the WLA liquefaction susceptibility analysis.

Geotechnical Borehole Data

Logs of geotechnical, groundwater, and environmental boreholes were compiled to provide geotechnical (e.g. penetration resistance, dry unit weight, plasticity, etc.) and lithologic (e.g. soil type, color, texture, particle-size distribution, etc.) data for shallow subsurface deposits in the Inner Valley (Kelson *et al.,* 1999). The WLA study used data from 159 boreholes, primarily from New Mexico State Highway and Transportation Department (NMSHTD) geotechnical investigations of highways and bridge crossings I compiled for the database included in this project. Additional data from 217 borehole logs were obtained by WLA from the New Mexico Environment Department (NMED), the City of Albuquerque (COA), the United States Geological Survey (USGS) Water Resources Division, United States Army Corps of Engineers (USACOE), New Mexico Office of the State Engineer (NMOSE), Albuquerque Metropolitan Arroyo Flood Control Authority, and private consulting firms. The additional borehole data obtained by WLA were later compiled and included in the database presented in my study (Chapter 3). Many of the boreholes in the database are from sites containing multiple boreholes, so representative boreholes from each site were chosen by WLA for their analyses. The

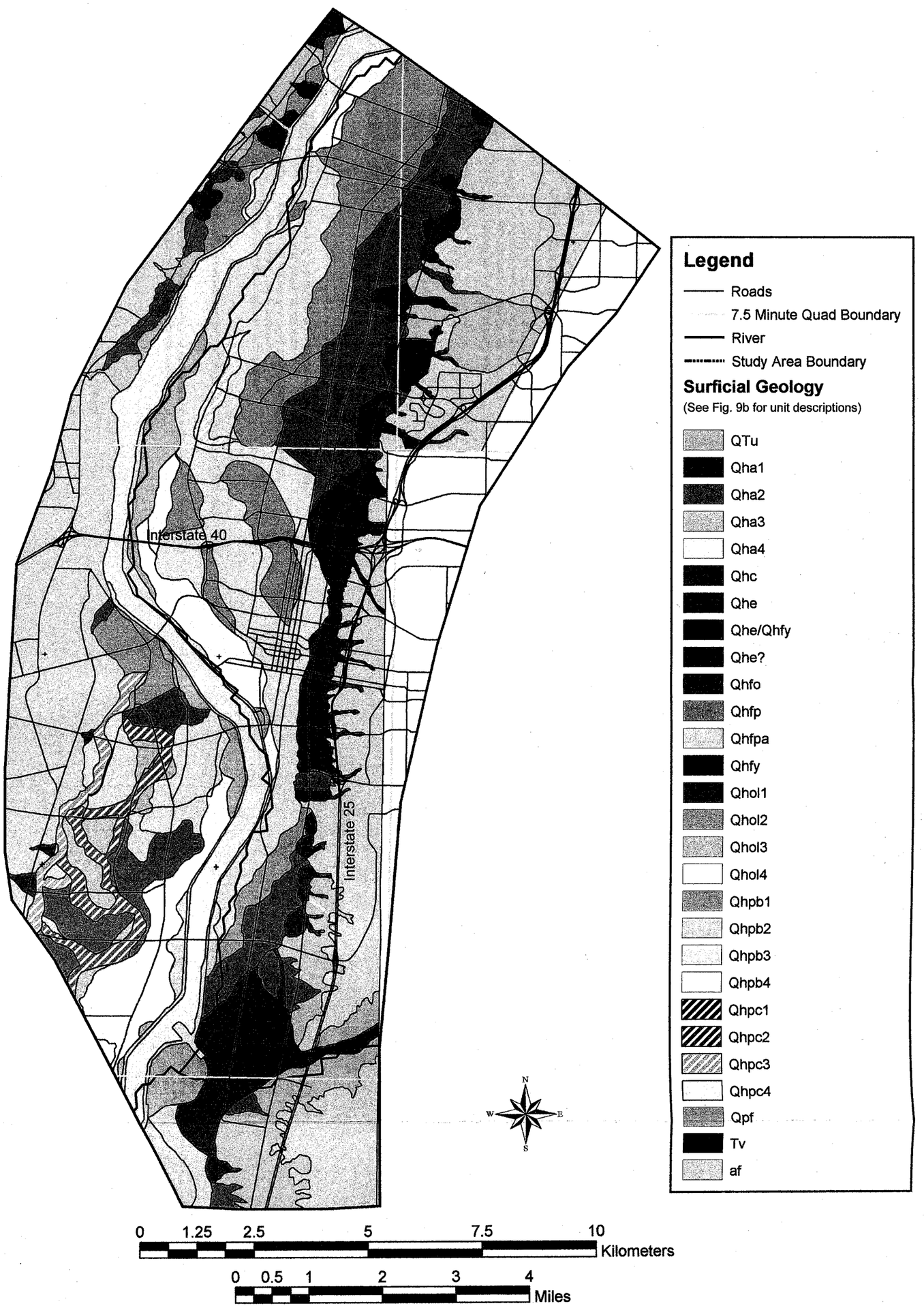

Figure 9a. Map showing Quaternary surficial geology used by WLA for liquefaction susceptibility analysis. This figure shows WLA map clipped to the boundary of this study area (modified from Kelson *et al.*, 1999).

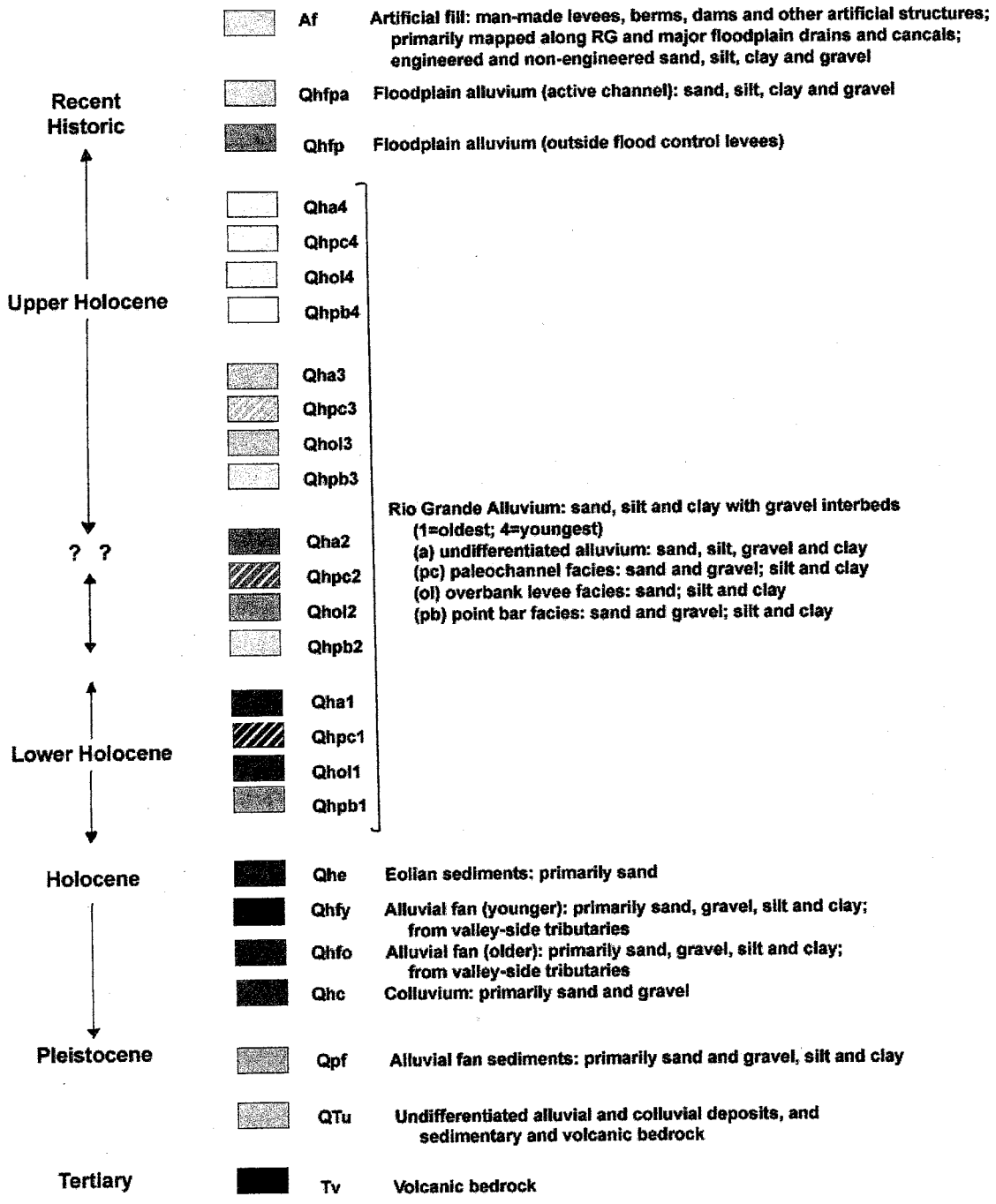

Figure 9b. Key to surficial geology and unit descriptions

final analyses were conducted using data from 243 boreholes representing approximately 75 sites (Kelson *et al.,* 1999).

Depth to Groundwater Map

The depth to groundwater map used in the WLA approach was created based on the compilation of data from numerous sources including a water well and monitoring well database developed by the USGS Water Resources Division, from depth to water measurements recorded in borehole logs as described above, and from water level data in open drainage ditches excavated by the Middle Rio Grande Conservancy District (MRGCD; Kelson *et al.,* 1999). Only water depth data from wells that had screened intervals above 100 feet and drive point wells (10 feet depth) throughout the study area were used to determine shallow water levels. Only these shallow water levels were used because depth to groundwater is a significant factor in determining liquefaction susceptibility and liquefaction generally occurs in saturated sediments less than 40 ft (12 m) below the ground surface. Determining depth to shallow groundwater was complicated locally by water-table declines due to groundwater withdrawal and seasonal fluctuations. WLA chose to construct depth to water maps that represent a conservatively shallow historic maximum water table that may not characterize present day groundwater depths, but will provide a worst-case scenario in evaluating liquefaction susceptibility (Figure 10).

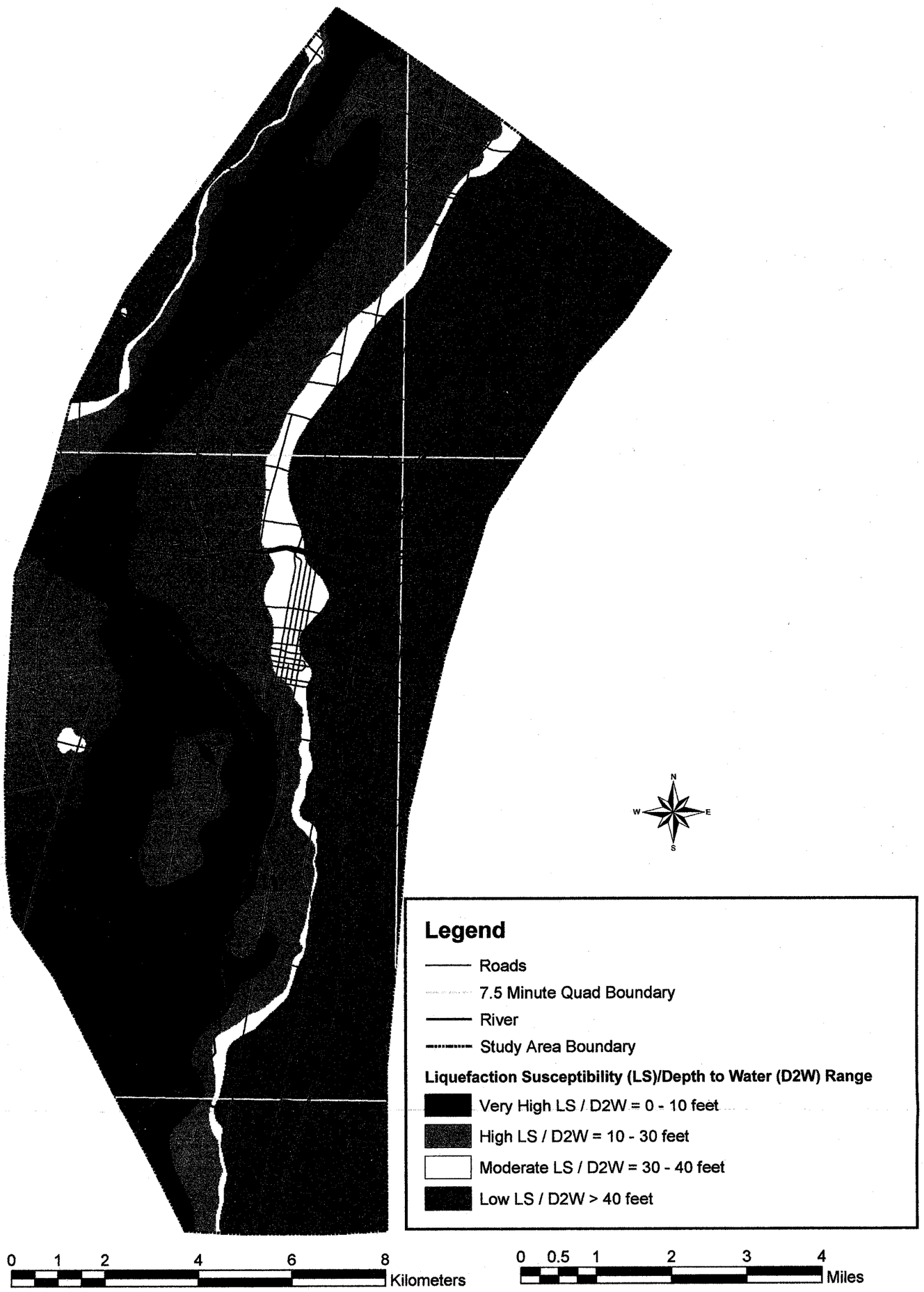

Figure 10. Map showing WLA depth to water reclassified as liquefaction susceptibility ranking.

Liquefaction Susceptibility Map

WLA used a two-fold approach to developing a liquefaction susceptibility map dependent on the presence or absence of geotechnical borehole data . If geotechnical data existed for the borehole, liquefaction susceptibility was determined based on the Liquefaction Threshold Analysis portion of Figure 11; otherwise it was based on the Geologic Criteria portion. The Liquefaction Threshold Analysis relies on the total thickness of loose sandy deposits within 40 ft (12m) of the ground surface, depth to groundwater, and the estimated threshold ground motion required to initiate liquefaction (Kelson *et al.,* 1999). Calculations of the threshold ground motions are based on standardized SPT blow count data ($(N_1)_{60}$) and results of the Seed Simplified Procedure (SSP) for a large (M=7.0) magnitude earthquake. Susceptibility rankings (Very High to Very Low) are determined by the peak horizontal ground acceleration (PGA) triggers shown below:

Very High – may trigger liquefaction at less than 0.1 g

High – may trigger liquefaction between 0.1 g and 0.2 g

Moderate – may trigger liquefaction between 0.2 g and 0.3 g

Low – may trigger liquefaction at levels above 0.3 g

Very Low – unlikely to trigger liquefaction at any level of acceleration

The Geologic Criteria analysis relies on the relative age and texture of the deposit as described on surficial geologic maps, depth to groundwater, and similarity to deposits

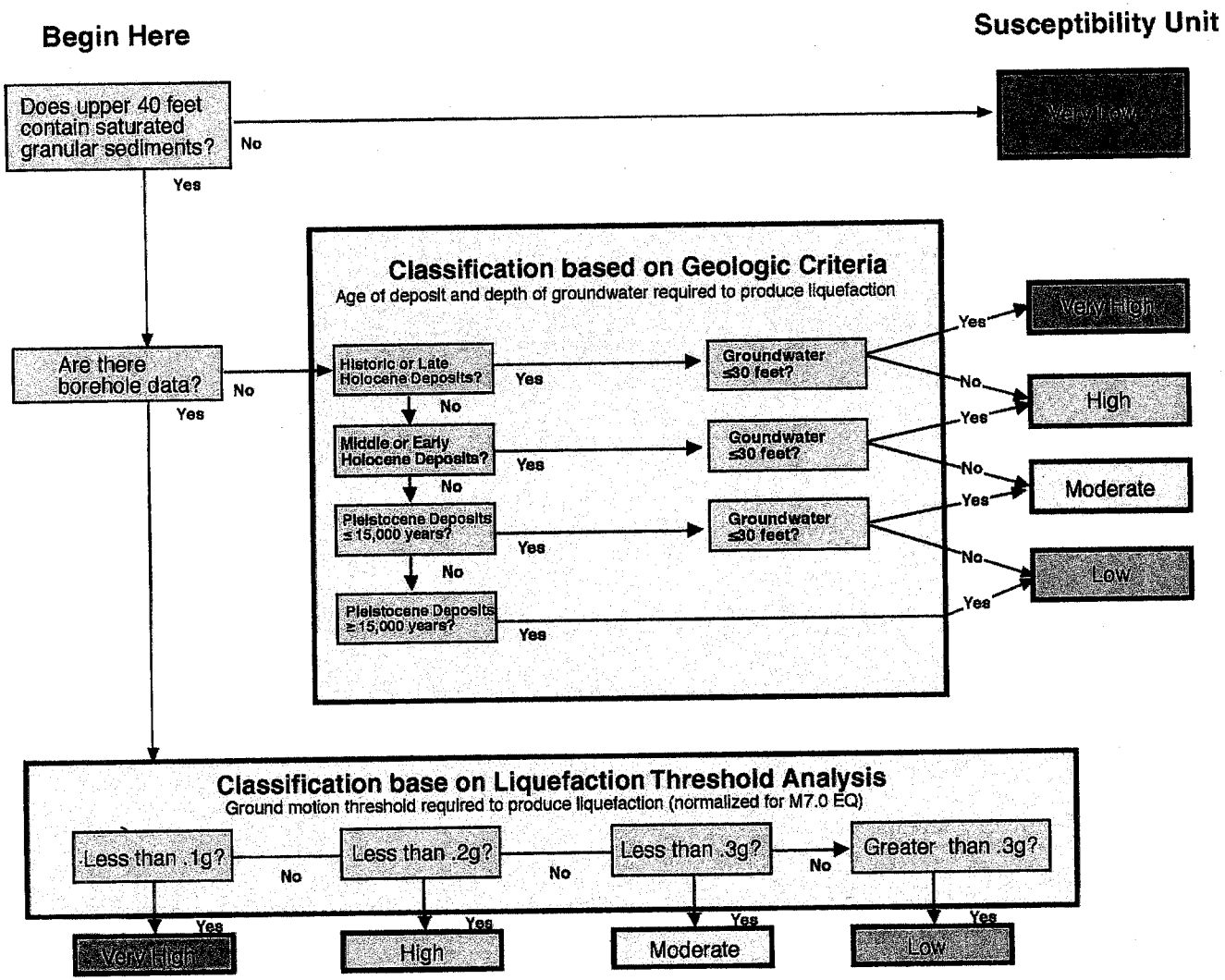

Figure 11. WLA flow chart for evaluating liquefaction susceptibility (Kelson *et al.*, 1999).

for which borehole classification was applied (Kelson *et al.,* 1999). Relative ages can be used when sufficient borehole data are not available because older deposits are typically more compacted and less susceptible to liquefaction. Table 4 summarizes the liquefaction susceptibility criteria matrix used in the WLA analysis. The final liquefaction susceptibility map developed by WLA is shown in Figure 12.

Table 4. WLA method criteria for assigning liquefaction susceptibility rankings for the Albuquerque, New Mexico area (from Kelson *et al.*, 1999).

Geologic Unit	Description	Range in Ground Motion Threshold (g) *	Number of Analyses	Mean Ground Motion Threshold (g) **	Liquefaction Susceptibility Class per Groundwater Depth		
					< 30'	30' - 40'	> 40'
Af	Artificial fill (Recent)	no data	none	no data	VH	H	L
Qhfpa, Qhfp	Floodplain Deposits (latest Holocene to Recent)	0.03 to 0.26	41	0.12 + 0.06	VH	H	L
Qha4	Valley Alluvial Deposits (all facies, late Holocene)	0.03 to 0.15	9	0.11 + 0.03	H	M	L
Qha3	Valley Alluvial Deposits (all facies, late Holocene)	0.05 to 0.20	25	0.13 + 0.05	H	M	L
Qha2	Valley Alluvial Deposits (all facies, late Holocene)	0.08 to 0.21	12	0.14 + 0.04	H	M	L
Qha1	Valley Alluvial Deposits (all facies, middle Holocene)	0.20 to 0.30	4	0.28 + 0.04	H	M	L
Qhe	Eolian Deposits (early to late Holocene)	no data	none	no data	H	M	L
Qhfy	Alluvial Fan Deposits (late Holocene)	0.07 to 0.20	6	0.17 + 0.05	H	M	L
Qhfo	Alluvial Fan Deposits (early to middle Holocene)	no data	none	no data	H	M	L
Qhc	Colluvial Deposits (early to late Holocene)	no data	none	no data	M	L	L
Qpf	Alluvial Fan Deposits (late Pleistocene)	no data	none	no data	M	L	L
QTu	Rio Grande alluvium and Santa Fe Group (undifferentiated, Tertiary to middle Pleistocene)	0.20 to 0.50	6	0.28 + 0.11	L	L	VL
Tv	Bedrock (Tertiary)	no data	none	no data	VL	VL	VL

* Estimated peak ground acceleration (PGA) required to trigger liquefaction
** Mean +/- 2 standard deviations
H Liquefaction Susceptibility Class (**VH**=Very High, **H**=High, **M**=Moderate, **L**=Low, **VL**=Very Low)

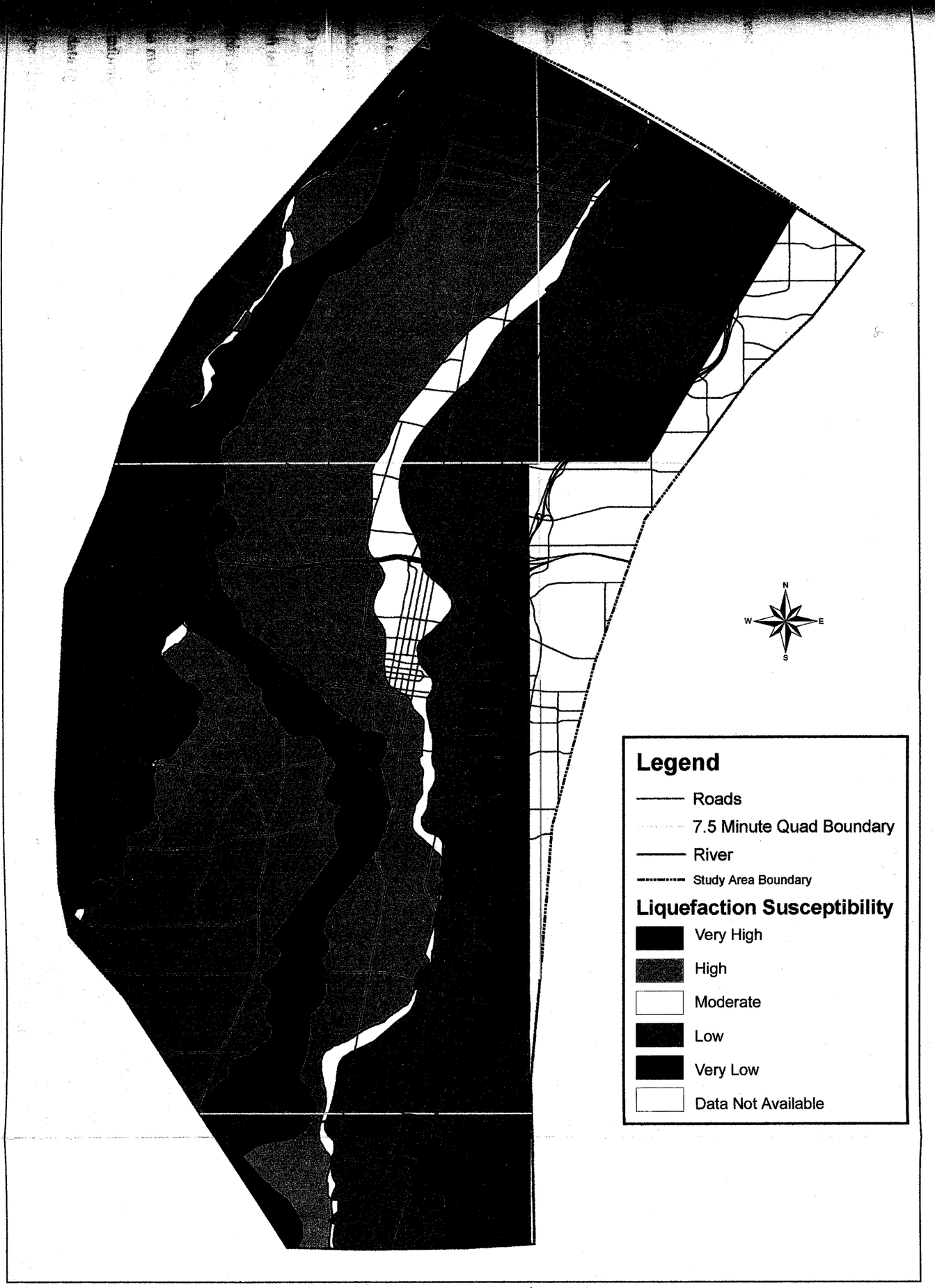

Figure 12. WLA liquefaction susceptibility map clipped to the boundary of this study area (modified from Kelson *et al.*, 1999).

CHAPTER 3. CURRENT STUDY

3.1 Database

The first step of this project was to create a database of shallow borehole information pertinent to engineering geologic and liquefaction susceptibility analyses for the Quaternary alluvium in the study area. This database was designed in Microsoft Access 97 and then converted to Microsoft Access 2000. A digital copy of the database is located on the included CD-ROM. The database is divided into four separate tables: Index, Location, Grain Size, and Geotech. The tables contain the data categories shown in Figure 13. The Index and Location tables have a one-to-one relationship. Each unique borehole ID number is linked to itself in the other table. However, the Grain Size and Geotech tables have a one-to-many relationship with the Index table. Each unique borehole ID number in the Index table is linked to many of the same in the Grain Size and Geotech tables to encompass all depth intervals for each boring.

Within this database the quality of information varies from borehole to borehole. Much of the information was taken directly from drillers' logs. In some cases, it was necessary to make interpretations based on information given in other borehole logs. The amount of information for each borehole is not consistent, either. Some sources provide laboratory data (grain size, geotechnical) and others provide only a verbal description of sediment type. There are also varying

DATABASE STRUCTURE			
INDEX	**LOCATION**	**GEOTECH**	**GRAIN SIZE**
ID#	Borehole ID #	Borehole ID #	Borehole ID #
Borehole ID #	UTM Easting	Depth (Top)	Depth (Top)
Well ID	UTM Northing	Depth (Bottom)	Depth (Bottom)
Location (UTM Easting)	NM State Plane (Easting)	SPT 1	Moisture
Location (UTM Northing)	NM State Plane (Northing)	SPT 2	Consistency
Type of Boring	Verbal	SPT 3	Color
Type of data		SPT N-Value	Texture
Visual/Lab Classification		Water Content	AASHTO Classification
Ground Elevation		Liquid Limit	USCS Classification
Depth to Water		Plasticity Index	*U.S. Standard Sieves*
Total Depth of Well		Density (dry)	3"
Source		Density (wet)	2"
		Cohesion	1"
		Angle of Internal Friction	3/4"
		Specific Gravity	1/2"
			3/8"
			No. 4
			No. 10
			No. 40
			No. 200

Figure 13. Format of borehole information database.

levels of accuracy in the location information provided for each borehole. Some logs include surveyed coordinate locations while the coordinates for others were determined from plotted approximations of location based on sketches and location information provided with the borehole data and are only accurate to ±100 ft (25 m). Other boreholes were not included in the liquefaction susceptibility analyses presented in the following section due to insufficient location information, but a general verbal location for these is given in the Location table. The database contains available data for 407 boreholes.

3.2 Spatial Distribution of Soils

Several lithologic logs showing the distribution of soils across the study area are shown along lines plotted on Figure 14. Line A-A' (Figure 15) extends roughly North-South in the northern part of the study area; line B-B' (Figure 16) is from WNW-ESE; line C-C' (Figure 17) is NNW-SSE in the southern portion of the study area. All of these areas show a high degree of spatial variability in grain size and sorting. The most complete West to East dataset is along Interstate-40 from the Bridge over the Rio Grande to Sixth Street. These data are shown along line D-D' (Figure 18).

In a fluvial depositional environment, one would expect to see less spatial variability parallel to the river and much more spatial variability perpendicular to the river. These trends are not easy to see in the figures, as the sparse nature of the available data does not allow a detailed analysis of the anisotropy and lateral persistence of the soils. The lines cover distances ranging from approximately 4,000 to 13,000 meters and have elevation changes ranging from 1.5 to 15 meters. It is, however, evident in the

Figure 14. Map showing locations of all data points and section lines.

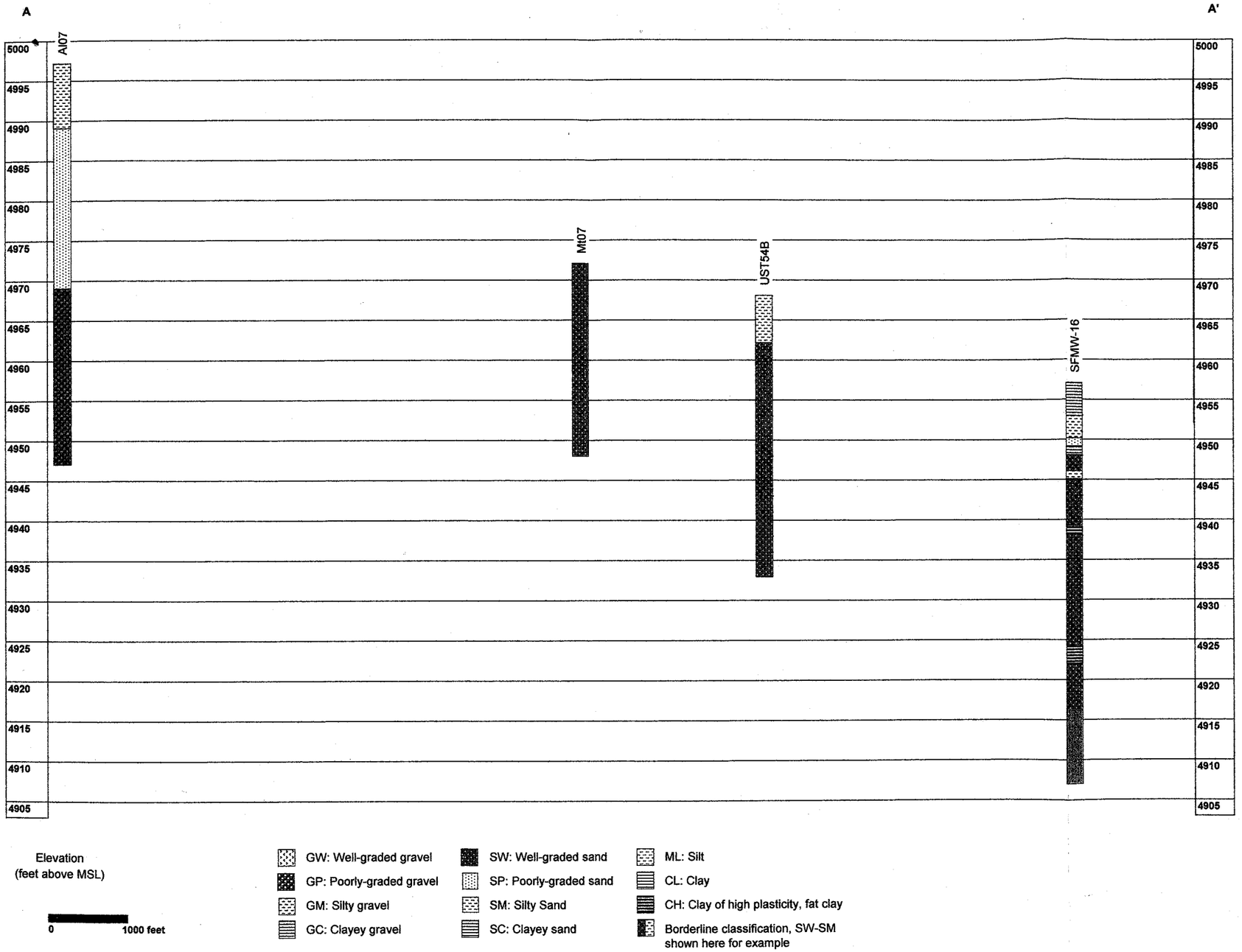

Figure 15. Lithologic logs along line A-A', location shown on Figure 14. Tops of logs are at ground surface.

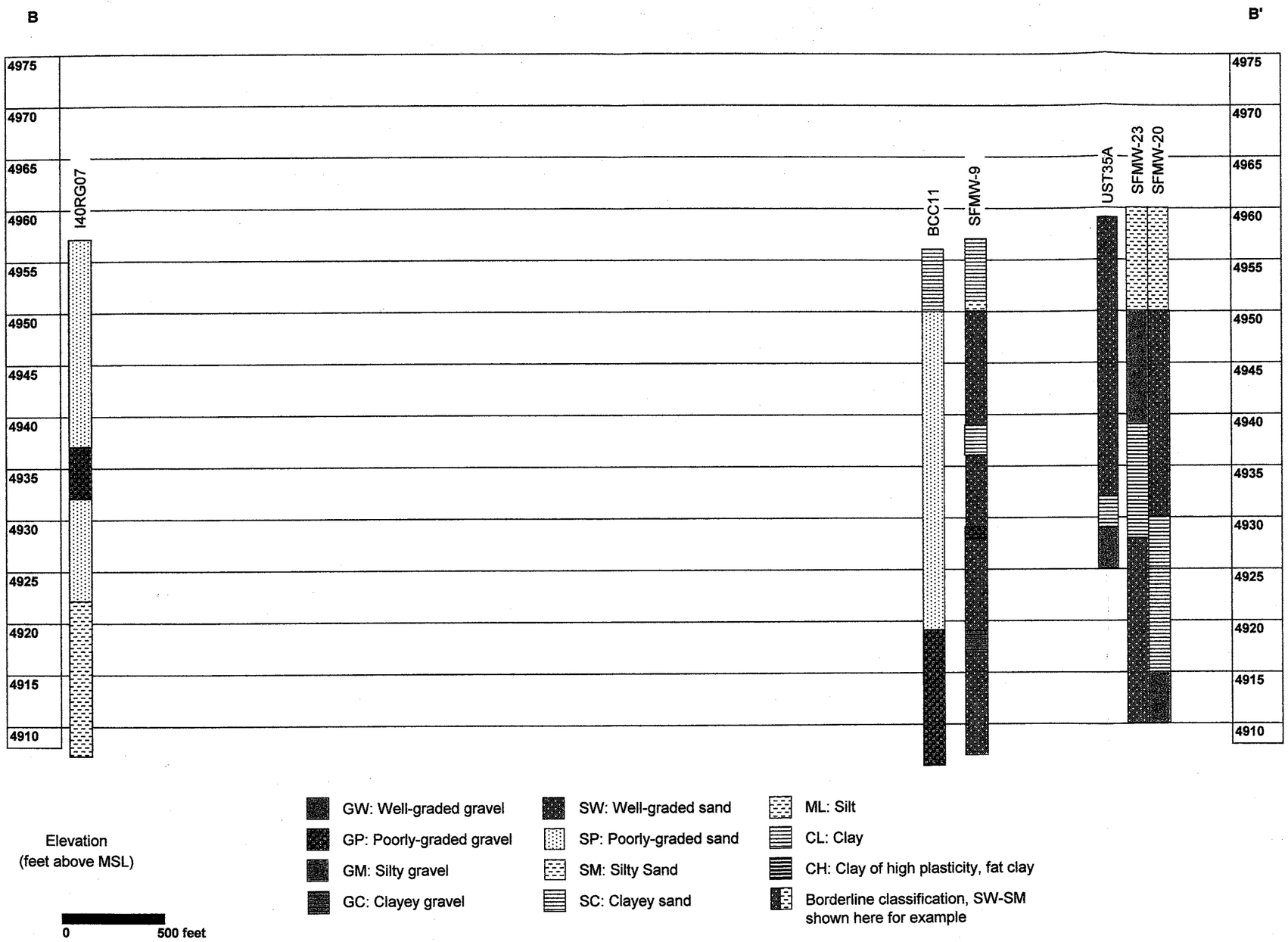

Figure 16. Lithologic logs along line B-B', location shown on Figure 14. Tops of logs are at ground surface.

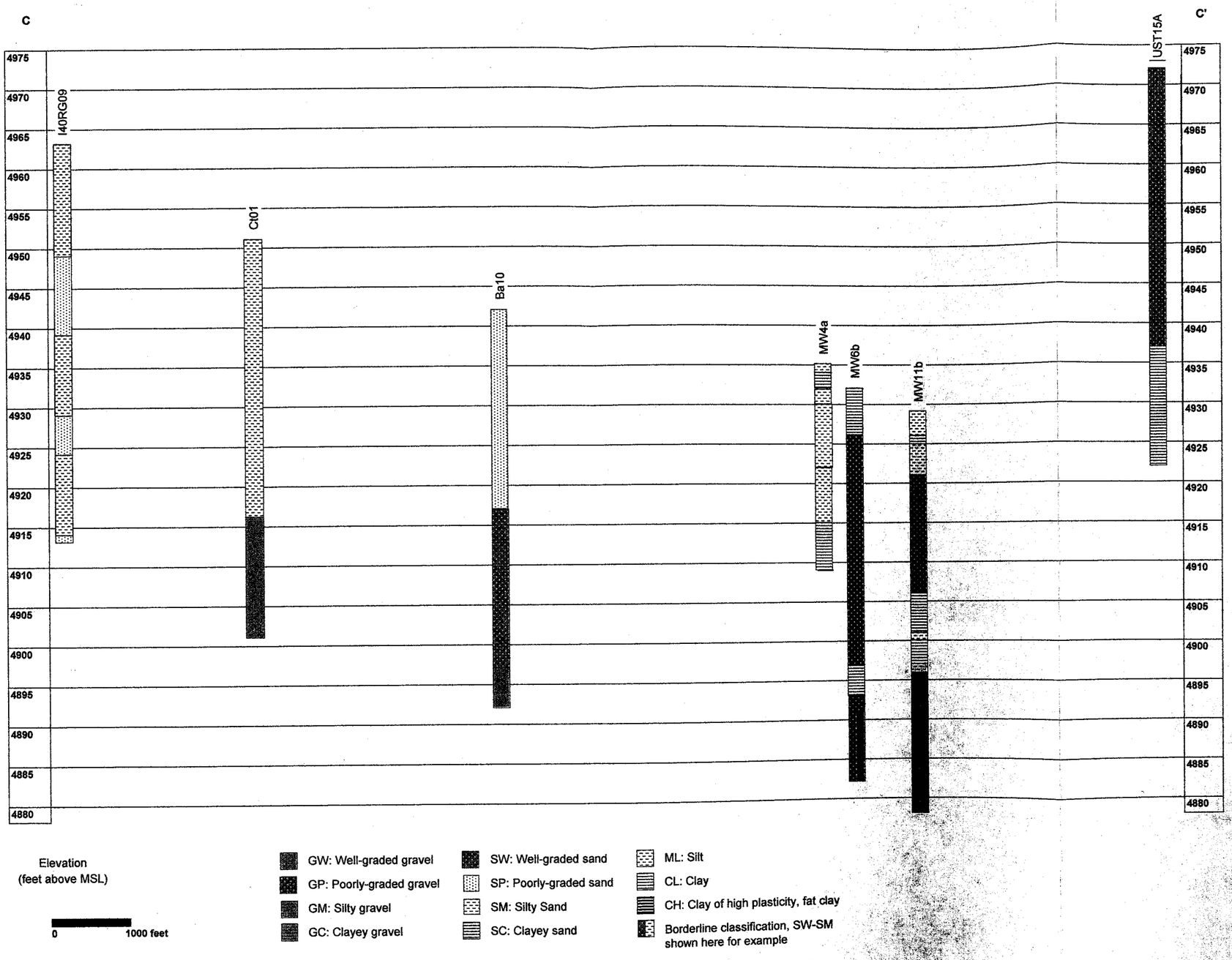

Figure 17. Lithologic logs along line C-C', location shown on Figure 14. Tops of logs are at ground surface.

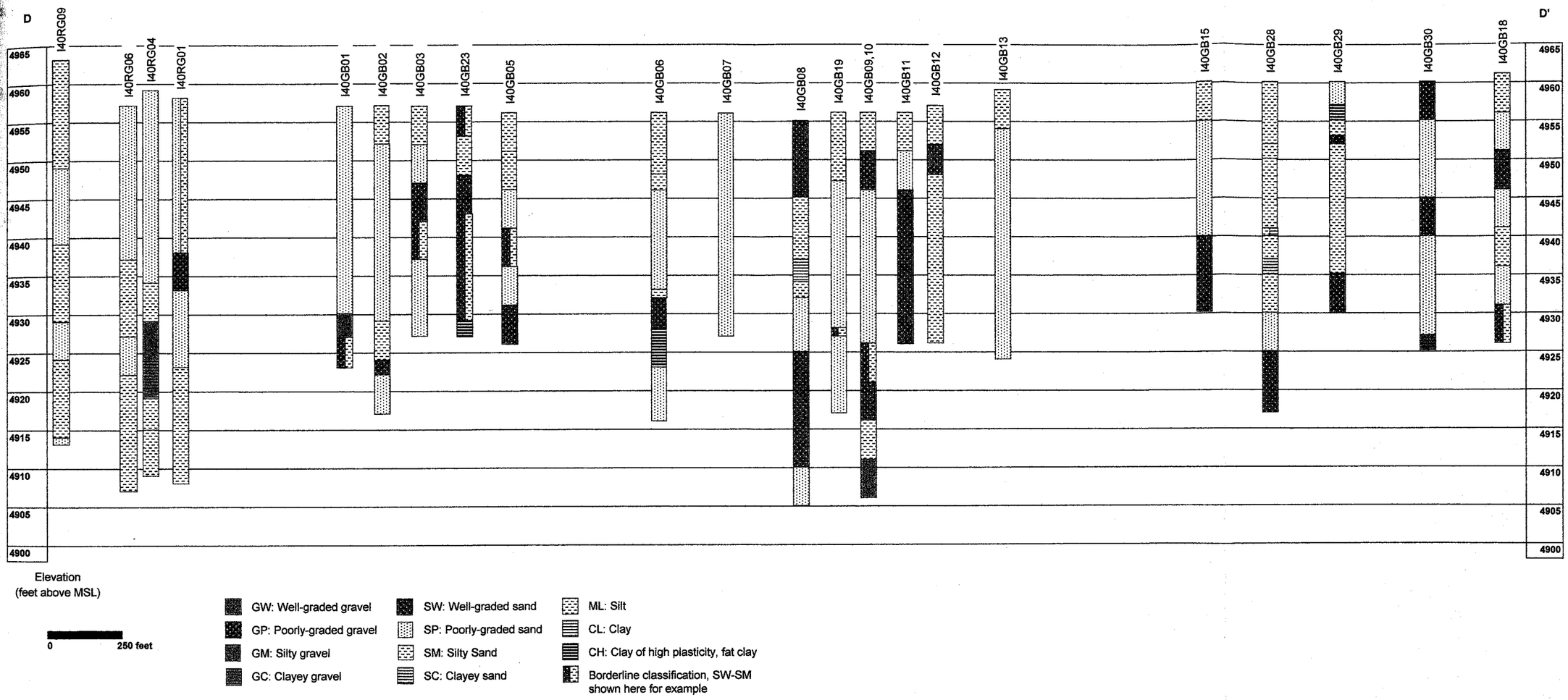

Figure 18. Lithologic logs along line D-D', location shown on Figure 14. Tops of logs are at ground surface.

figures that sands with lesser amounts of gravels, silts, and clays dominate the study area, which is common in fluvial/alluvial environments. It is also important to note that there is significant variability in grain size and sorting with depth along all lines.

3.3 JAC Liquefaction Susceptibility Methods

JAC Methods A and B were designed as extensions of the method used by WLA (Kelson *et al.*, 1999) in an attempt to understand the role vertical variation in soil characteristics plays in the evaluation of liquefaction susceptibility. A cartoon diagram developed by Mabey (1997; Figure 19) illustrates the potential shortcomings of a surface-only approach to hazard analysis, such as identifying a uniform hazard due to uniform surficial geology even though the thickness and engineering properties of the unit vary significantly. This is a potential limitation of the method used by WLA (1999). JAC Method A was designed to address this issue. To provide consistency for comparison purposes, the depth to water map developed by WLA was used in this method. Also, all calculations of standardized SPT blow count ($(N_1)_{60}$), CSR, and PGA trigger were performed using a proprietary spreadsheet developed by WLA as a template. The calculations were modified only to bracket the results with minimum and maximum values as opposed to an average. The calculations in the WLA spreadsheet are all based on the Seed Simplified Procedure (SSP) and subsequent revisions, discussed in Chapter 2 (Seed and Idriss, 1971, 1982; Seed, 1979; Seed *et al.*, 1983, 1985; NRC, 1985; Seed and Harder, 1990; NCEER, 1997; Idriss, 1997; Robertson and Wride, 1997; Youd, 1997).

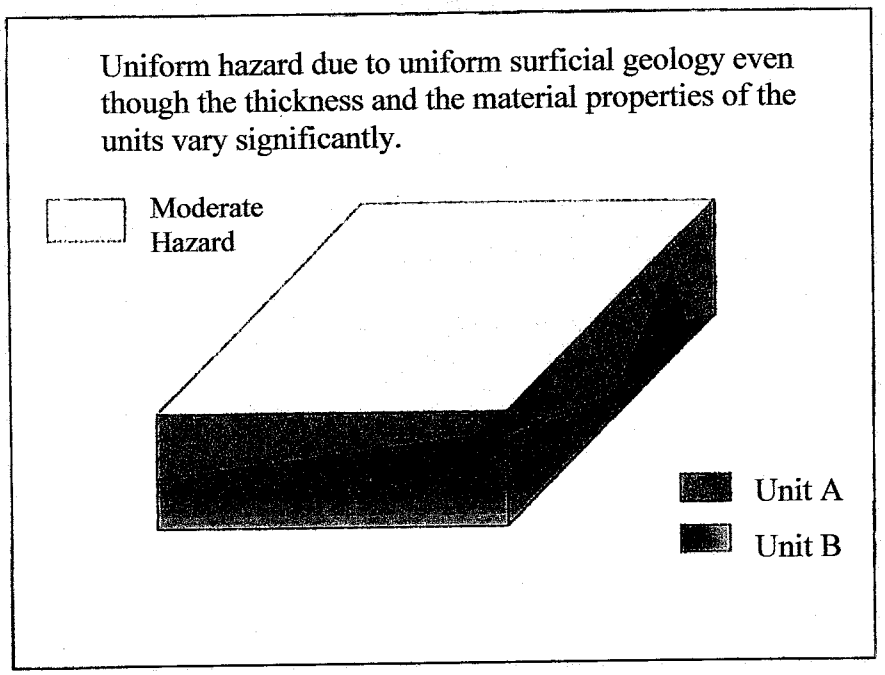

Figure 19. Block diagram showing potential shortcomings of surficial geologic map interpretation of liquefaction hazard (from Mabey, 1997). Units A and B have different material properties.

Once the calculations were complete for all available borehole data, minimum and maximum values for each of the three depth intervals were selected for each borehole. Instead of relying on geotechnical data alone, WLA used surficial geology to rank the susceptibility of units where borehole data were not available. However, since additional borehole data were compiled after the WLA study was completed, the JAC Methods relied solely on the borehole data and interpolations of the data were made at three depth intervals below ground surface: 1) 0 – 10 feet, 2) 10 – 30 feet, and 3) 30 – 40 feet. This allowed the spatial variability of the material properties of the sediments at depth to be considered.

JAC Method B was developed to estimate the result of using the standardized SPT blow count ($(N_1)_{60}$) data as opposed to the calculated PGA trigger in order to cut down on preprocessing calculation time. If these results share similar liquefaction susceptibility distributions, Method B would be a more efficient approach to evaluating liquefaction susceptibility over large regions.

As mentioned previously, all data included in the database were compiled directly from drillers' logs and engineering reports, and values were not available for all fields for all boreholes. Data required for evaluating liquefaction susceptibility using methods described in detail below include percent fines (percent passing No. 200 sieve), measured SPT blow counts, dry density/soil unit weight, and depth to water. These properties are either used directly from the database or combined to calculate other pertinent criteria such as peak ground acceleration (PGA) trigger. Available data were queried out of the database and expanded tables were created to include information derived from the following interpretations. For boreholes where percent fines data were not included in

the database the minimum and maximum percent fines were determined by comparing Unified Soil Classification System (USCS; Table 5) to information presented in Table 6. In cases where the USCS classification was not known, it could be determined by using the AASHTO (American Association of State Highway and Transportation Officials) classification (if given in the driller's log) or verbal description using the comparisons in Table 5. Measured SPT blow counts were compiled directly from the drillers' logs and engineering reports. Dry density/soil unit weight ranges were approximated using USCS classification and information in Table 6.

Tables containing Universal Transverse Mercator (UTM) eastings and northings and minimum and maximum percent fines, minimum and maximum standardized SPT blow counts ((N1)60), and minimum and maximum PGA trigger were exported from Microsoft Excel in DBF 4 (dbase iv) format for each of three depth intervals 1) 0 – 10 feet, 2) 10 – 30 feet, and 3) 30 – 40 feet. These "dbf" files were then imported as point coverages and projected to UTM NAD83 using the ArcToolbox software. The depth to groundwater map (Figure 10) developed by Kelson et al. (1999) was digitized, imported as a line coverage, and projected to UTM NAD83.

The data for this project were not evenly distributed across the study area; therefore, it was necessary to develop a means of interpolating the data across areas where there was little or no coverage. Geostatistical analyses were performed outside of the GIS software using GSLib (Deutsch and Journel, 1998), Variowin (Pannatier, 1996), and GS+ (Robertson, 2000) to determine whether correlations between data sets across the study area could be made. Unfortunately, the geostatistical analyses failed to provide suitable interpolations of the data, because the datasets were sparse and highly clustered

Table 5. Unified soil classification system with comparison to verbal description and AASHTO classification.

Unified Soil Classification System (USCS) [a]				Verbal Description	AASHTO Classification [b]
Major Divisions			Group Symbol	Group Name [a]	Most Probable Comparable Soil Groups
Coarse-grained soils - more than 50% retained on No. 200 sieve	Gravel - more than 50% of coarse fraction retained on No. 4 sieve	Clean Gravel	GW	Well-graded gravel, fine to coarse gravel	A-1-a
			GP	Poorly graded gravel	A-1-a
		Gravel with Fines	GM	Silty gravel	A-1-b, A-2-4, A-2-5, A-2-7
			GC	Clayey gravel	A-2-6, A-2-7
	Sand - more than 50% of coarse fraction passes on No. 4 sieve	Clean Sand	SW	Well-graded sand, fine to coarse sand	A-1-b
			SP	Poorly graded sand	A-3, A-1-b
		Sand with Fines	SM	Silty sand	A-1-b, A-2-4, A-2-5, A-2-7
			SC	Clayey sand	A-2-6, A-2-7
Fine-grained soils - more than 50% passes on No. 200 sieve	Silt and Clay - Liquid Limit less than 50	Inorganic	ML	Silt	A-4, A-5
			CL	Clay	A-6, A-7-6
		Organic	OL	Organic Silt, Organic Clay	A-4, A-5
	Silt and Clay - Liquid Limit 50 or more	Inorganic	MH	Silt of high plasticity, elastic silt	A-7-5, A-5
			CH	Clay of high plasticity, fat clay	A-7-6
		Organic	OH	Organic Clay, Organic Silt	A-7-5, A-5
Highly Organic Soils			PT	Peat	--

[a] ASTM, 1985
[b] Holtz and Kovacs, 1981

Table 6. Summary of minimum and maximum dry density/unit weight and percent fines values.

USCS Classification	Consistency	Dry Density/Unit Weight (γ_d) [pcf] [a]		Percent Fines [b]	
		Minimum	Maximum	Minimum	Maximum
GW	loose	98	130	0	5
GW	moderately dense	115	135	0	5
GW	dense to very dense	115	145	0	5
GP	loose	108	130	0	5
GP	moderately dense	115	130	0	5
GP	dense to very dense	111	134	0	5
GM	loose	51.5	130	12	45
GM	moderately dense	115	130	12	45
GM	dense to very dense	115	135	12	45
GC	dense to very dense	106	125	12	45
SW	loose	90	115	0	5
SW	moderately dense	90	119	0	5
SW	dense to very dense	90	130	0	5
SP	loose	88	115	0	5
SP	moderately dense	90	116	0	5
SP	dense to very dense	90	122	0	5
SM	loose	79.1	115	12	45
SM	moderately dense	63.7	119	12	45
SM	dense to very dense	70.5	128	12	45
SM		34	115	12	45
SC	dense to very dense	68	125	12	45
ML	loose	62.4	115	55	100
ML	moderately dense	86	115	55	100
ML	dense to very dense	92	120	55	100
ML		55.1	120	55	100
MH	all	48.4	115	55	100
Clays	very soft to soft	60	95	55	100
Clays	soft organic	30	50	55	100
Clays	medium	75	110	55	100
Clays	stiff to very stiff	90	130	55	100
Clays	with sand and gravel		135	55	100

[a] Hammond *et al.*, 1992 and Koloski *et al.*, 1989

[b] Holtz and Kovacs, 1981

(Figure 14). Results inconsistent with the actual data distribution were also encountered when using inverse distance weighting and spline methods. Therefore, other interpolation methods were evaluated. The *topogrid* command in ArcInfo yielded more geologically reasonable interpolations of the data, and allowed for the development of a complete GIS based spatial analysis approach. An explanation of the procedure used by the *topogrid* command can be found in Appendix A.

Another diagram by Mabey (1997; Figure 20) illustrates the potential shortcomings of using interpolation to develop hazard distributions. In an attempt to offset the uncertainty and bias inherent in the JAC methods a best case (least conservative) and worst case (most conservative) analysis was done to bracket the results. In this way, the results are interpreted as guidelines and not absolutes. If a site has a high potential for liquefaction in both the best and worst case scenarios then it should definitely be considered high and a more thorough site specific analysis should be completed based upon the proposed use of the site. However, if a site has a low potential for liquefaction in the best case scenario and a high potential in the worst case scenario, it is a situation with large uncertainty and should be evaluated in more detail according to the proposed use of the site.

Grids based on the line coverage of depth to water, and the point coverages of minimum and maximum percent fines, minimum and maximum standardized SPT blow counts ((N1)60), and minimum and maximum PGA trigger were created for each of three depth intervals 1) 0 – 10 feet, 2) 10 – 30 feet, and 3) 30 – 40 feet using the ArcInfo *topogrid* command. Each of these grids was then reclassified using ArcMap's Spatial Analyst extension. Reclassification is a process that allows certain vales or a range of

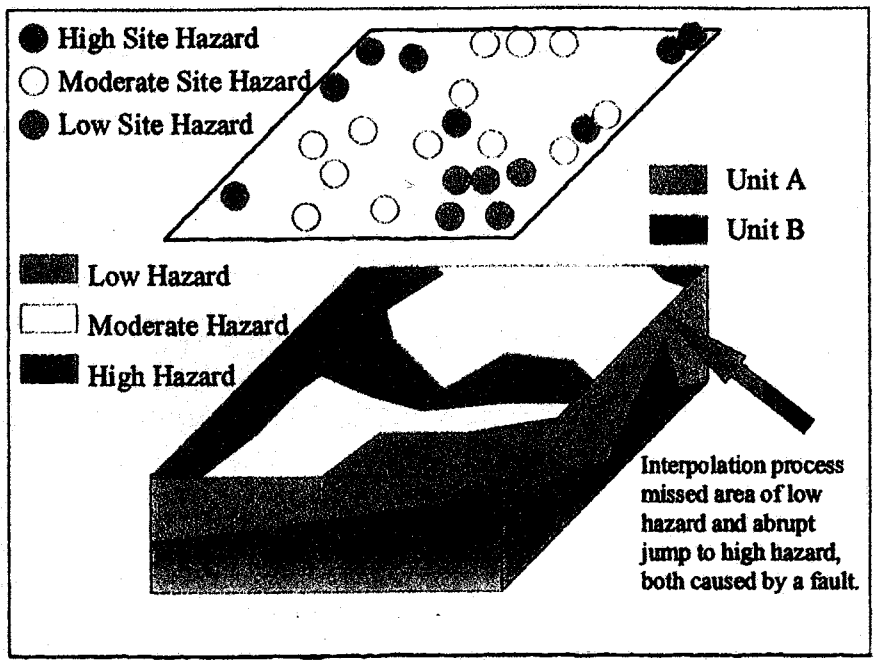

Figure 20. Block diagram illustrating the potential for incorrect evaluation of liquefaction hazard when based on interpolation of data (from Mabey, 1997).

values to be defined by another value. Figure 21 shows a simple example of reclassification where altitude data are reclassified based on the criteria given in the legend. The reclassification criteria I used in this study were synthesized from the range of values presented by numerous researchers in the literature (Table 7; Seed and Idriss, 1982; Seed *et al.,* 1985; Hadj-Hamou and Elton, 1989; OH EPA, 1996; DMG, 1997; Hwang and Lin, 1997; Tosun and Ulusay, 1997; Youd, 1998; Kelson *et al.,* 1999). The specific reclassification criteria used in ArcGIS are shown in Table 8. Figure 22 shows the reclassified maps for minimum percent fines at each of the three depth intervals evaluated.

The reclassified data were then combined in order to create best and worst case scenario liquefaction susceptibility maps for each depth interval. The reclassified data grids were combined using the Map Algebra command in ArcMap's Spatial Analyst extension. Figure 23 shows a schematic example of how the MapAlgebra command was applied in this study. Figure 24 shows exactly what data were combined to create the best and worst case scenario liquefaction susceptibility maps at each depth interval for each method. Each of these liquefaction susceptibility maps was then reclassified based on the criteria in Table 9. The reclassified liquefaction susceptibility maps for each depth interval for each of the methods are shown in Figures 25-28. The next step in evaluating the liquefaction susceptibility was to then add each of the resultant depth interval grids together to create grids for overall best and worst case scenario liquefaction susceptibility for each of the two methods. Refer to Figure 24 for a diagram showing the grid relationships. The resultant grids had values ranging from three to fifteen. The final step was an additional reclassification based on the values shown in Table 9. This step

Altitude

100	110	225	150
10	300	210	30
15	390	250	30
10	10	30	20

Reclassified altitude

0	1	2	1
0	2	2	0
0	3	2	0
0	0	0	0

Legend	
Reclassified Value	Altitude
0	1 - 100 m.
1	101 - 200 m.
2	201 - 300 m.
3	301 - 400 m.

Figure 21. Example of a simple reclassification process. Each grid cell gets a new value based on reclassification criteria given in legend.

Table 7. Values used in GIS reclassification scheme based on literature review.

Reference	Criteria
Kelson *et al.*, 1999	Very High Liquefaction Susceptibility: May trigger at < 0.1g High Liquefaction Susceptibility: May trigger between 0.1g and 0.2 g Moderate Liquefaction Susceptibility: May trigger between 0.2 g and 0.3 g Low Liquefaction Susceptibility: May trigger at > 0.3g Very Low Liquefaction Susceptibility: Unlikely to trigger at < any level of acceleration
Seed *et al.*, 1995	Liquefaction not likely if corrected SPT N-Value > 22
Maecuson *et al.*, 1990	Liquefaction not likely if corrected SPT N-Value > 30
Hwang and Lin, 1997	Liquefaction is likely if: Depth soil < 20 m (~66 ft) Depth groundwater < 10 m (~33 ft) SPT N-values < 20
Tosun and Ulusay, 1997	Liquefaction is not likely if: SPT N-values > 25 Fines > 35%
Ohio EPA, 1996	Potential for liquefaction decreases with increase in fines content If Clay content > 20% will not liquefy unless extremely sensitive Full saturation is generally necessary

Table 8. Reclassification criteria used in ArcMap for percent fines, peak ground acceleration (PGA), standardized SPT blow counts ($SPT(N_1)_{60}$), and depth to water.

Percent Fines	PGA (g)	$SPT(N_1)_{60}$	Depth to Water (ft)	Relative Liquefaction Susceptibility	Interpretation of Relative Liquefaction Susceptibility values
0 - 5	0 - 0.1	0 - 9	0 - 10	1	Very High
5 - 15	0.1 - 0.2	9 - 16	10 - 30	2	High
15 - 25	0.2 - 0.3	16 - 23	30 - 40	3	Moderate
25 - 35	> 0.3	23 - 30	> 40	4	Low
35 - 100		> 30		5	Very Low

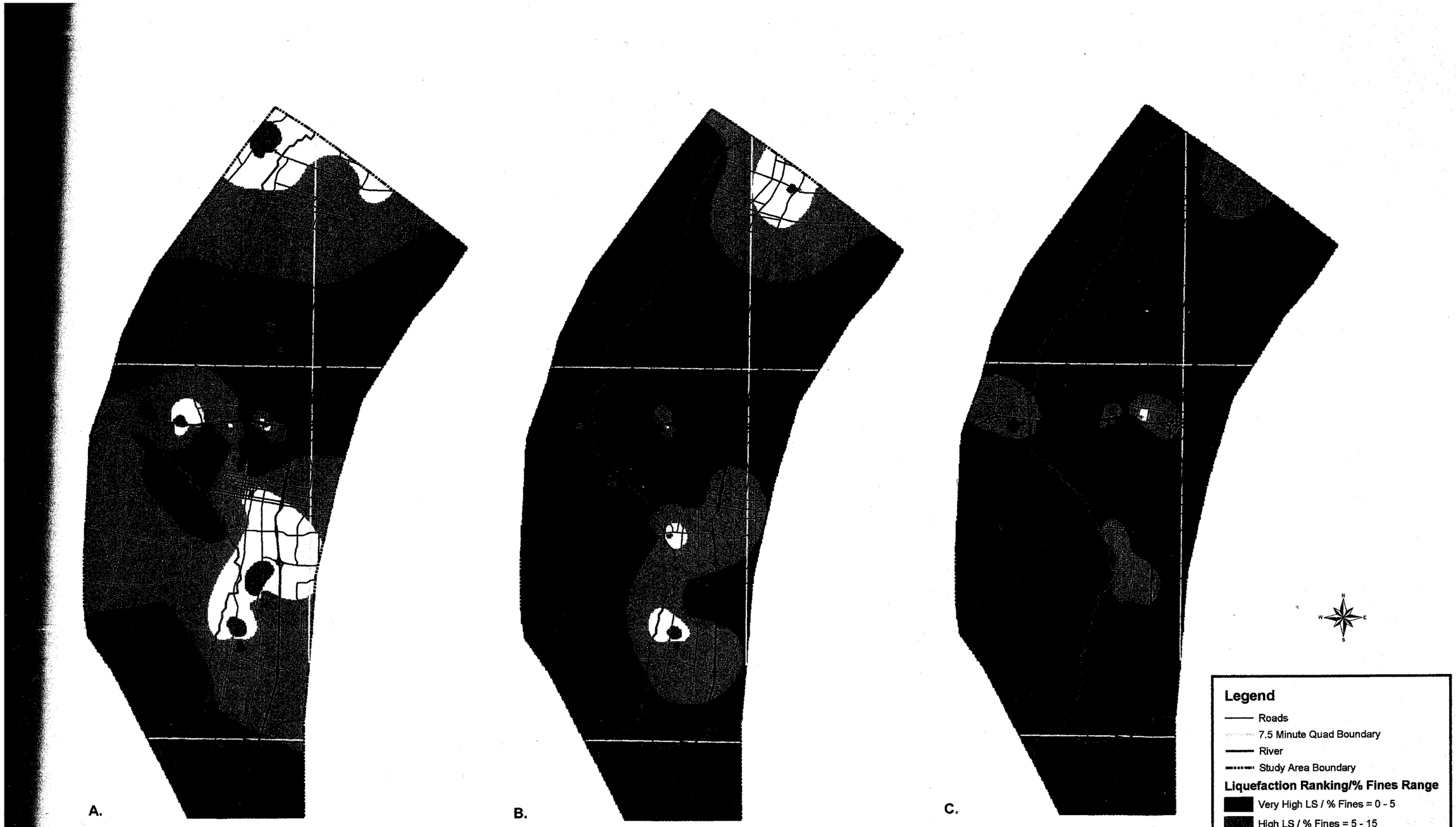

Figure 22. Reclassified maps of minimum percent fines for three depth intervals A. 0 - 10 feet, B. 10 - 30 feet, and C. 30 - 40 feet.

1	1	3
4	5	2
3	3	2
3	4	5

Reclassified
Percent Fines

+

1	1	1
2	3	2
3	3	2
4	4	3

Reclassified
PGA

+

3	1	2
2	1	3
2	1	3
1	1	4

Reclassified
Depth to Water

=

5	3	6
8	9	7
8	7	7
8	9	12

Liquefaction Susceptibility

Figure 23. Schematic example of MapAlgebra command as used in this study. The values in each grid cell are added to get a total value for that grid cell.

Depth Interval	JAC Method A				JAC Method B			
	Best Case Scenario		Worst Case Scenario		Best Case Scenario		Worst Case Scenario	
0 - 10 feet	reclassified percent fines maximum + reclassified PGA maximum + depth to water = Liquefaction susceptibility	+	reclassified percent fines minimum + reclassified PGA minimum + depth to water = Liquefaction susceptibility	+	reclassified percent fines maximum + reclassified SPT $(N_1)_{60}$ maximum + depth to water = Liquefaction susceptibility	+	reclassified percent fines minimum + reclassified SPT $(N_1)_{60}$ minimum + depth to water = Liquefaction susceptibility	+
10 - 30 feet	reclassified percent fines maximum + reclassified PGA maximum + depth to water = Liquefaction susceptibility	+	reclassified percent fines minimum + reclassified PGA minimum + depth to water = Liquefaction susceptibility	+	reclassified percent fines maximum + reclassified SPT $(N_1)_{60}$ maximum + depth to water = Liquefaction susceptibility	+	reclassified percent fines minimum + reclassified SPT $(N_1)_{60}$ minimum + depth to water = Liquefaction susceptibility	+
30 - 40 feet	reclassified percent fines maximum + reclassified PGA maximum + depth to water = Liquefaction susceptibility	=	reclassified percent fines minimum + reclassified PGA minimum + depth to water = Liquefaction susceptibility	=	reclassified percent fines maximum + reclassified SPT $(N_1)_{60}$ maximum + depth to water = Liquefaction susceptibility	=	reclassified percent fines minimum + reclassified SPT $(N_1)_{60}$ minimum + depth to water = Liquefaction susceptibility	=
Overall	Liquefaction susceptibility		Liquefaction susceptibility		Liquefaction susceptibility		Liquefaction susceptibility	

Figure 24. Diagram showing data layers and how they are combined for the JAC liquefaction susceptibility methods.

Table 9. Reclassification criteria for liquefaction susceptibility maps.

Sum of grids of relative liquefaction susceptibility	Relative Liquefaction Susceptibility	Interpretation of Relative Liquefaction Susceptibility values
3 - 4	1	Very High
5 - 7	2	High
8 - 10	3	Moderate
11 - 13	4	Low
14 - 15	5	Very Low

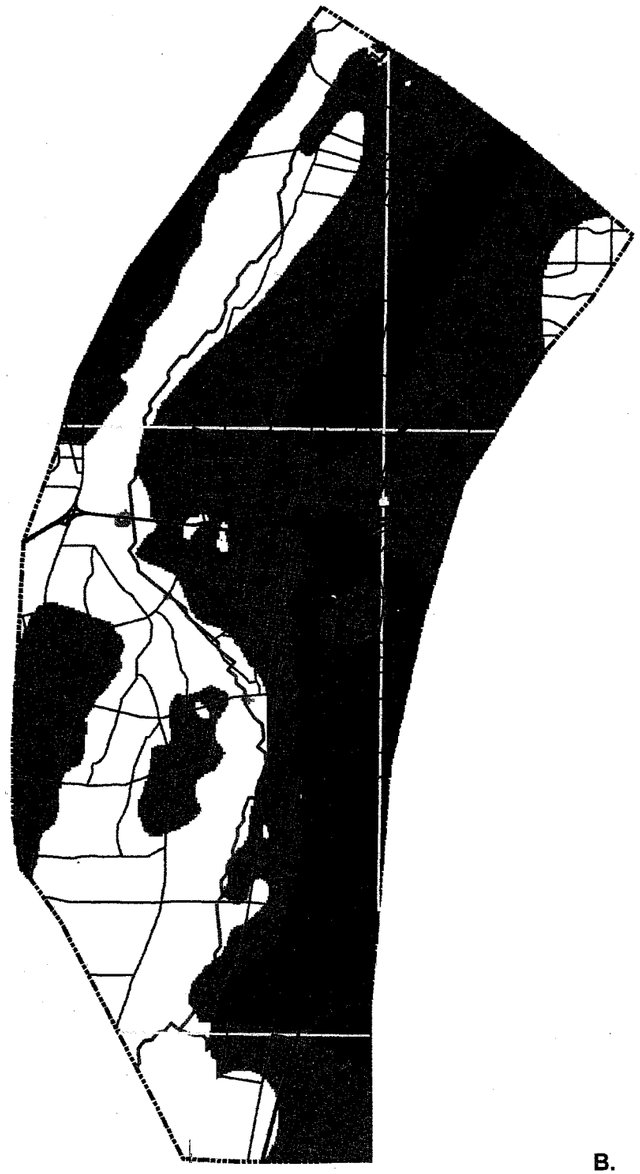

A.

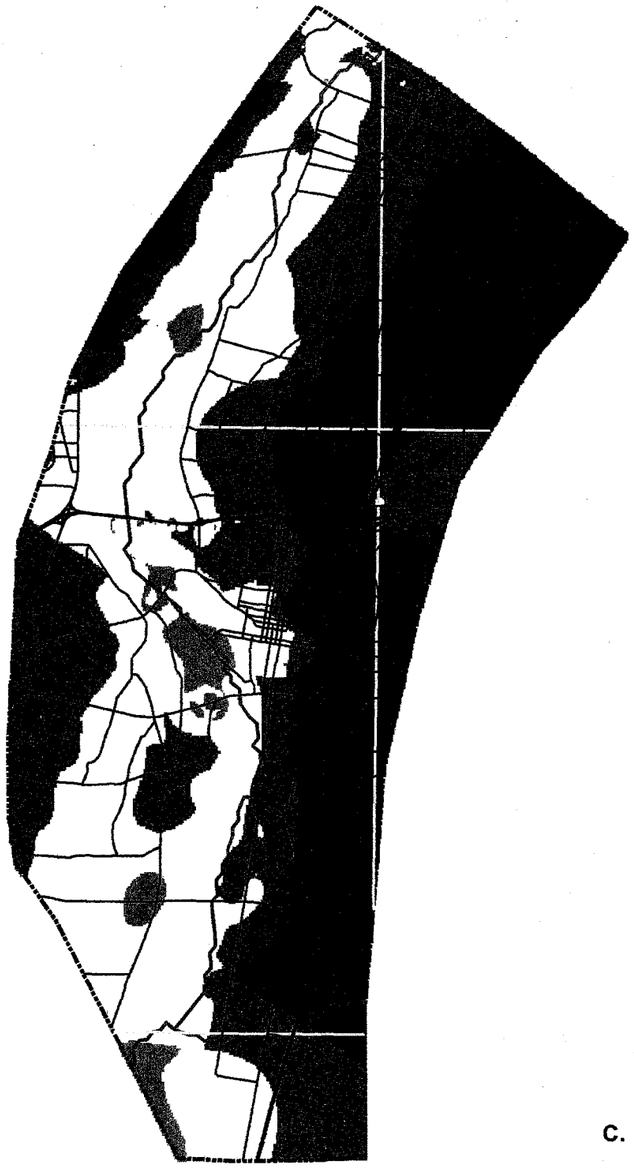

B.

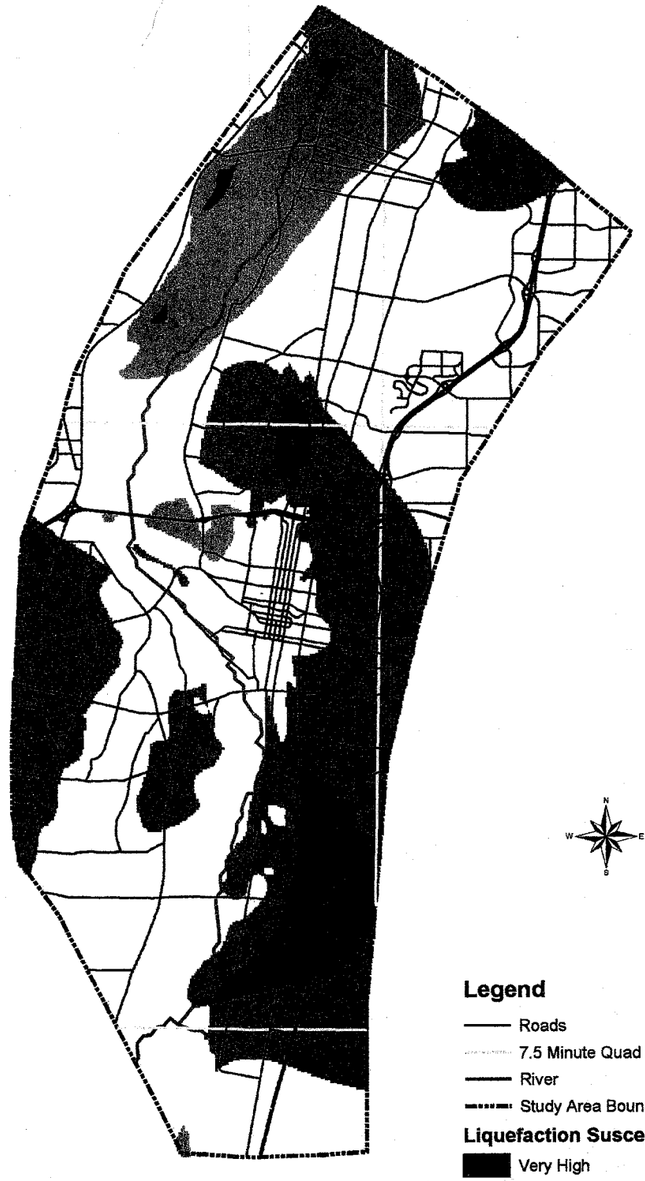

C.

0 1.25 2.5 5 7.5 10
Kilometers

0 0.5 1 2 3 4
Miles

N
W E
S

Legend

- Roads
- 7.5 Minute Quad Boundary
- River
- Study Area Boundary

Liquefaction Susceptibility

- Very High
- High
- Moderate
- Low
- Very Low

Figure 25. Reclassified maps of JAC Method A Best Case Scenario liquefaction susceptibility for three depth intervals A. 0 - 10 feet, B. 10 - 30 feet, and C. 30 - 40 feet.

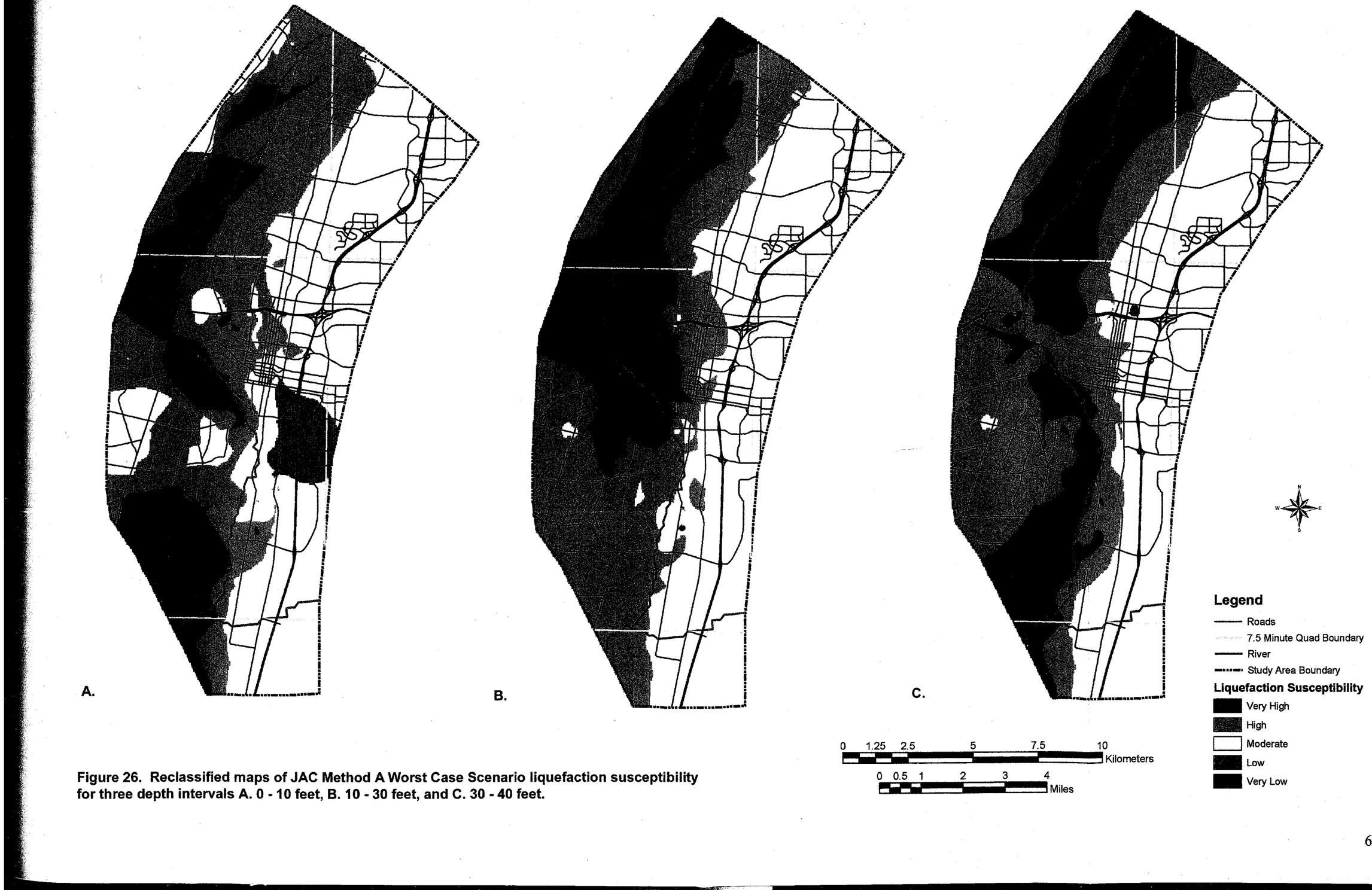

Figure 26. Reclassified maps of JAC Method A Worst Case Scenario liquefaction susceptibility for three depth intervals A. 0 - 10 feet, B. 10 - 30 feet, and C. 30 - 40 feet.

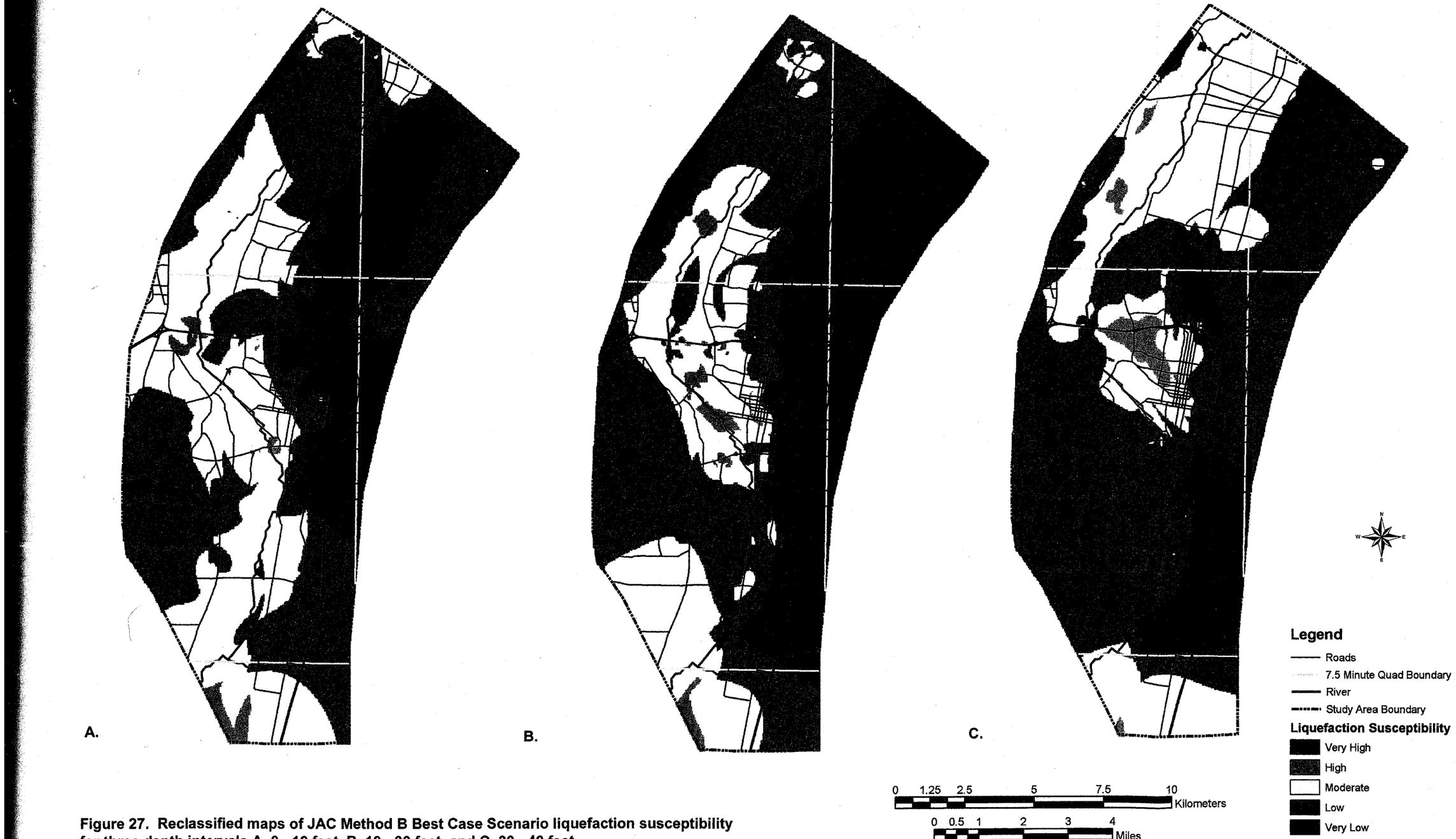

Figure 27. Reclassified maps of JAC Method B Best Case Scenario liquefaction susceptibility for three depth intervals A. 0 - 10 feet, B. 10 - 30 feet, and C. 30 - 40 feet.

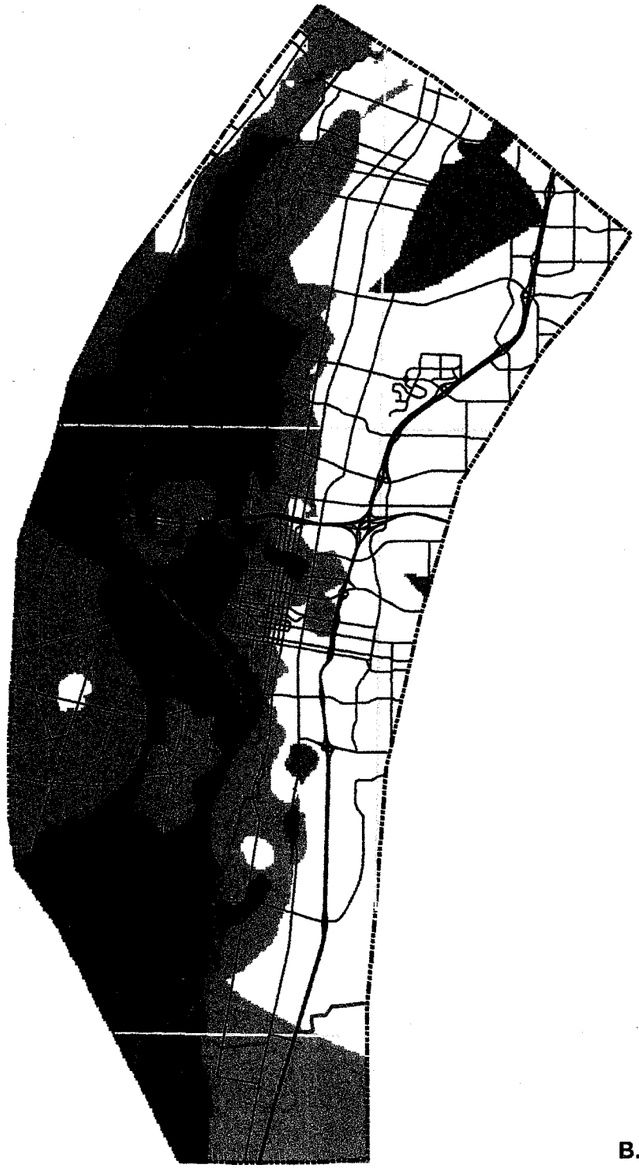

A.

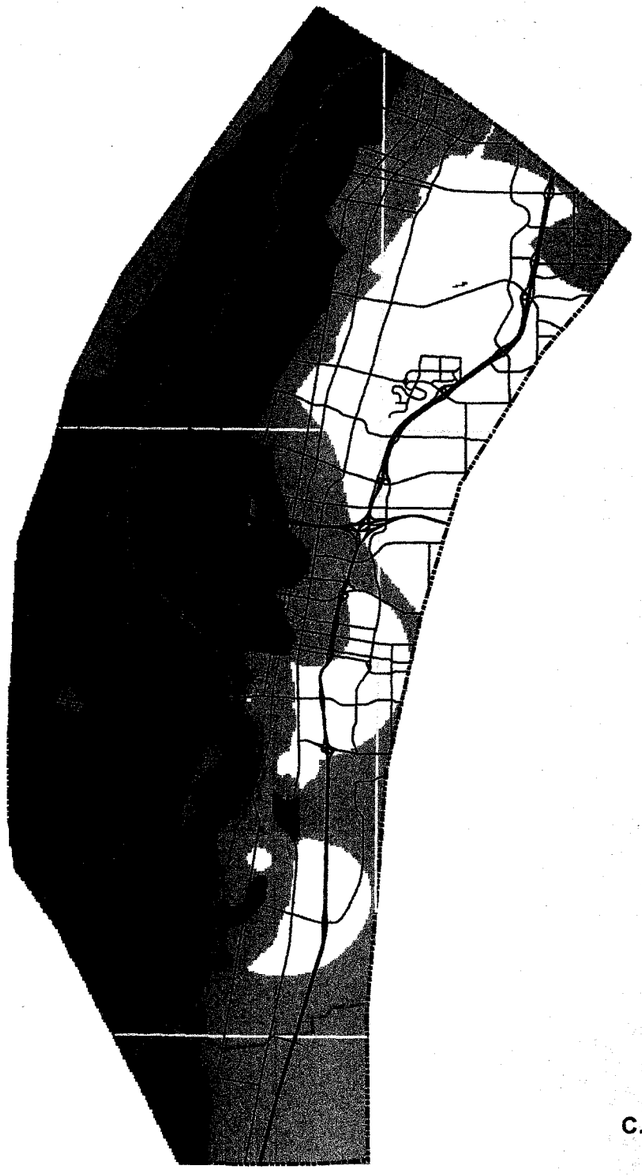

B.

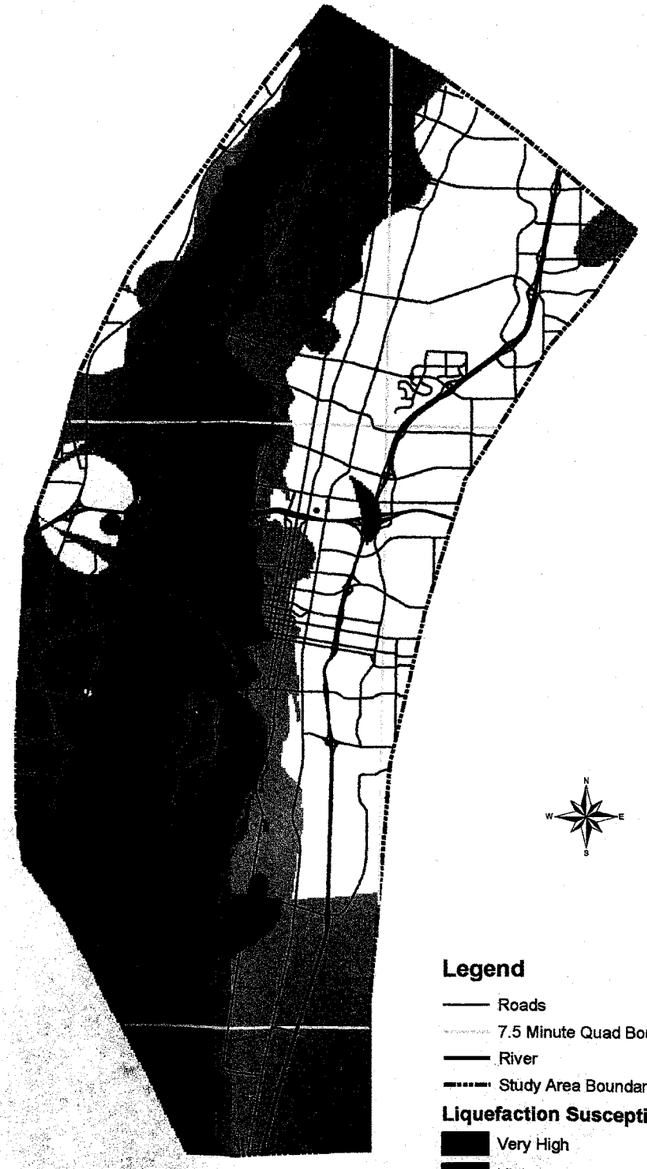

C.

0 1.25 2.5 5 7.5 10 Kilometers

0 0.5 1 2 3 4 Miles

N W E S

Legend

- Roads
- 7.5 Minute Quad Boundary
- River
- Study Area Boundary

Liquefaction Susceptibility

- Very High
- High
- Moderate
- Low
- Very Low

Figure 28. Reclassified maps of JAC Method B Worst Case Scenario liquefaction susceptibility for three depth intervals A. 0 - 10 feet, B. 10 - 30 feet, and C. 30 - 40 feet.

resulted in the final overall best and worst case scenario liquefaction susceptibility maps for each of the two methods (Figures 29-32).

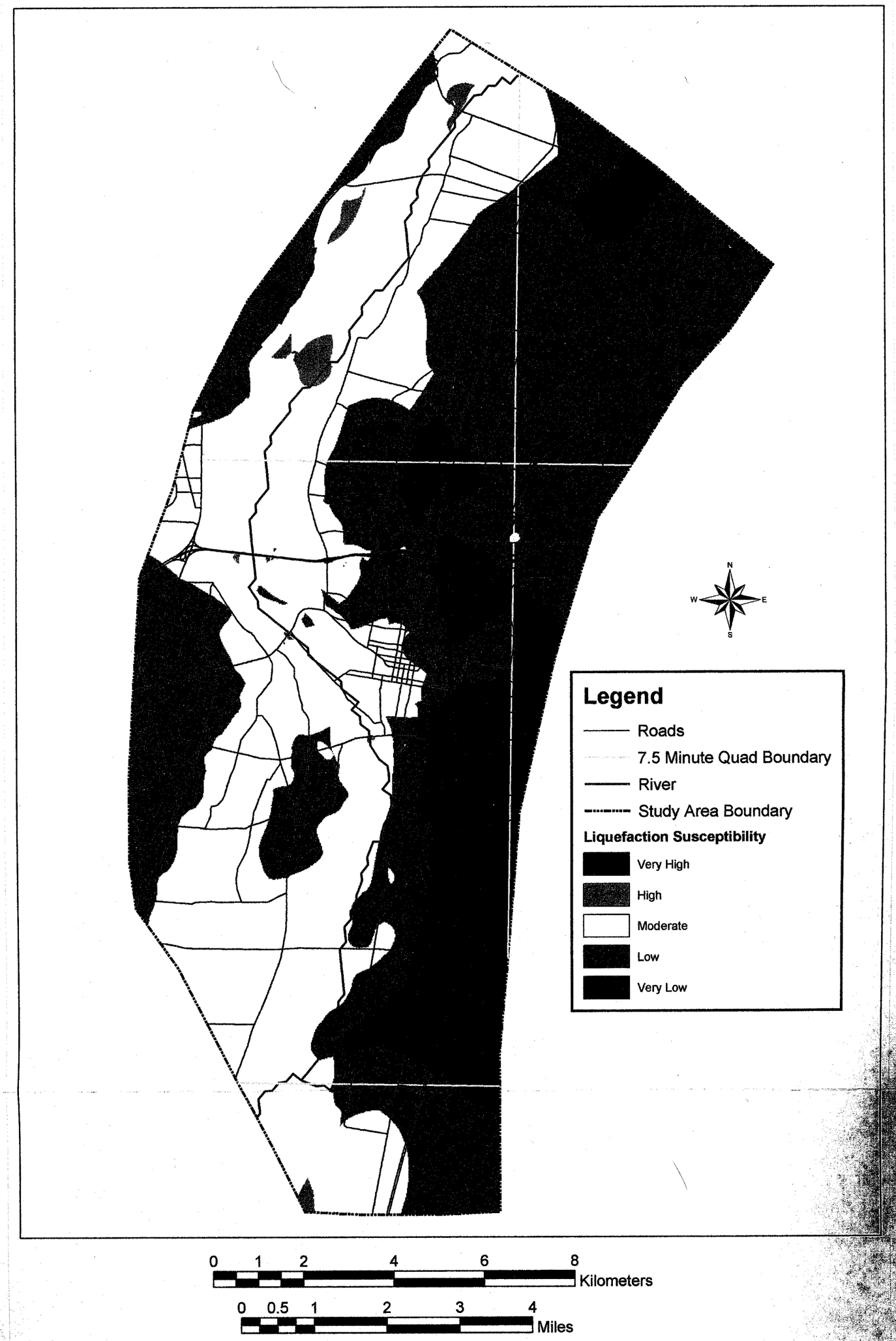

Figure 29. JAC Method A overall Best Case Scenario Liquefaction Susceptibility Map.

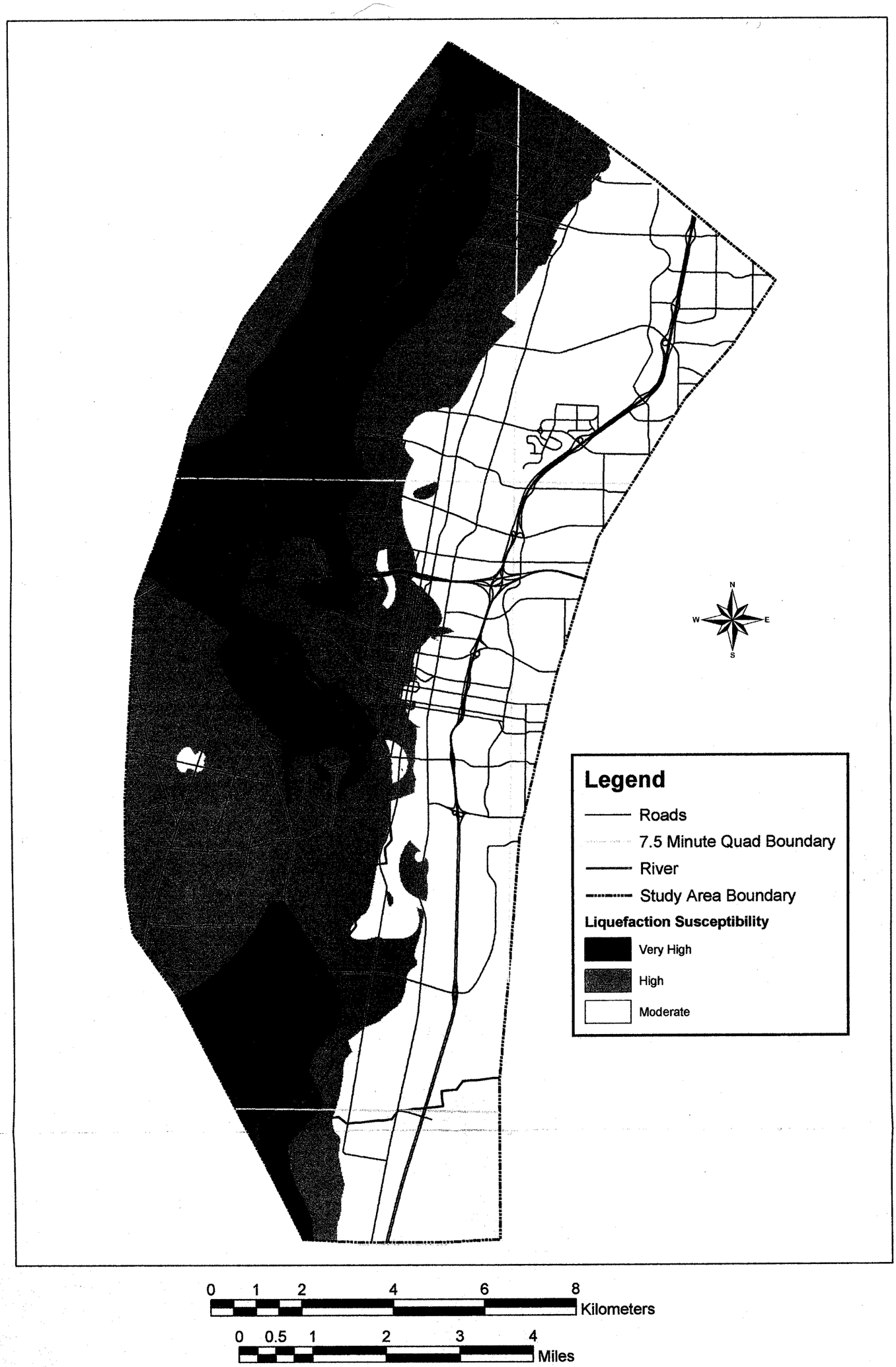

Figure 30. JAC Method A overall Worst Case Scenario Liquefaction Susceptibility Map.

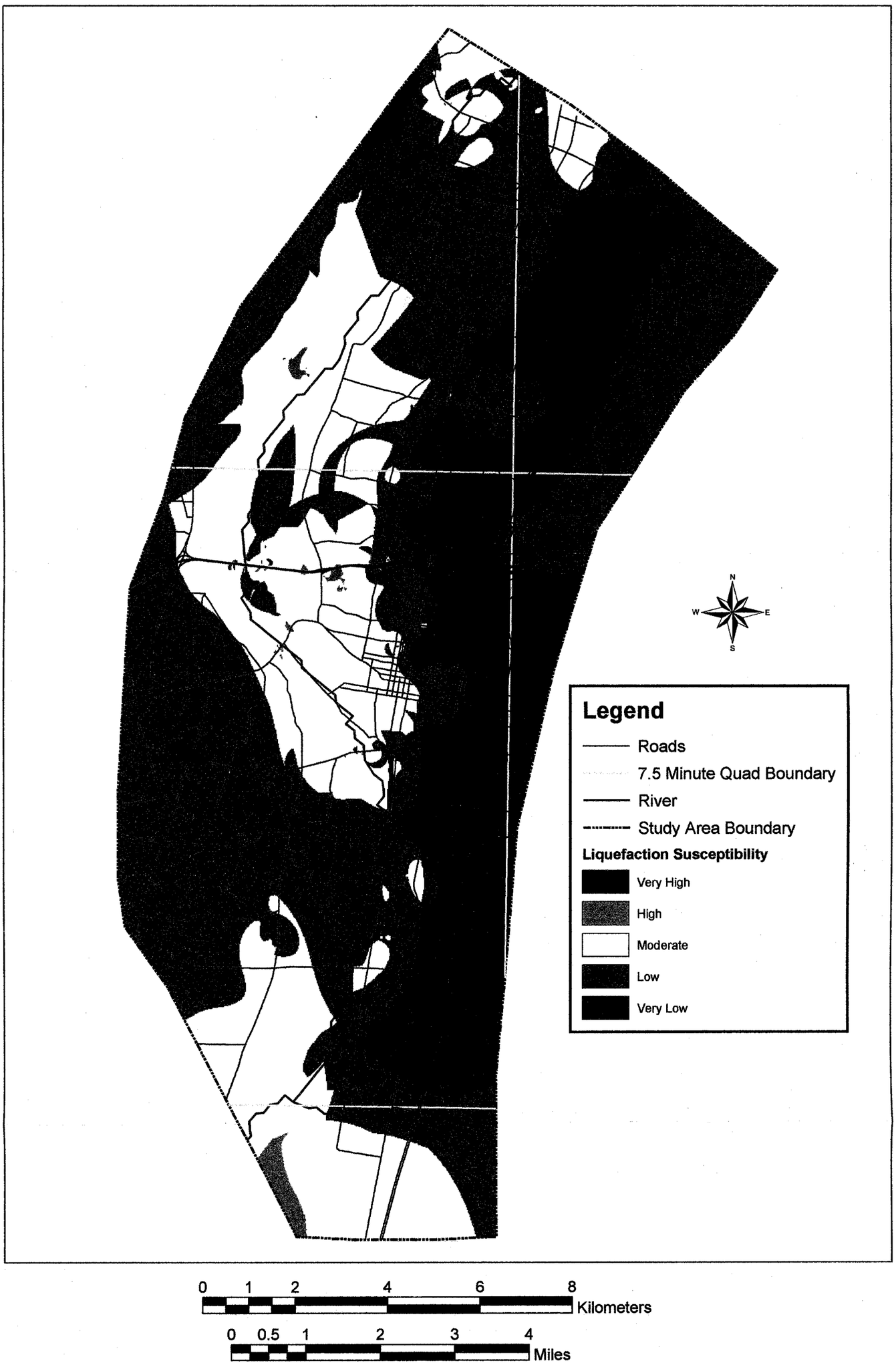

Figure 31. JAC Method B overall Best Case Scenario Liquefaction Susceptibility Map.

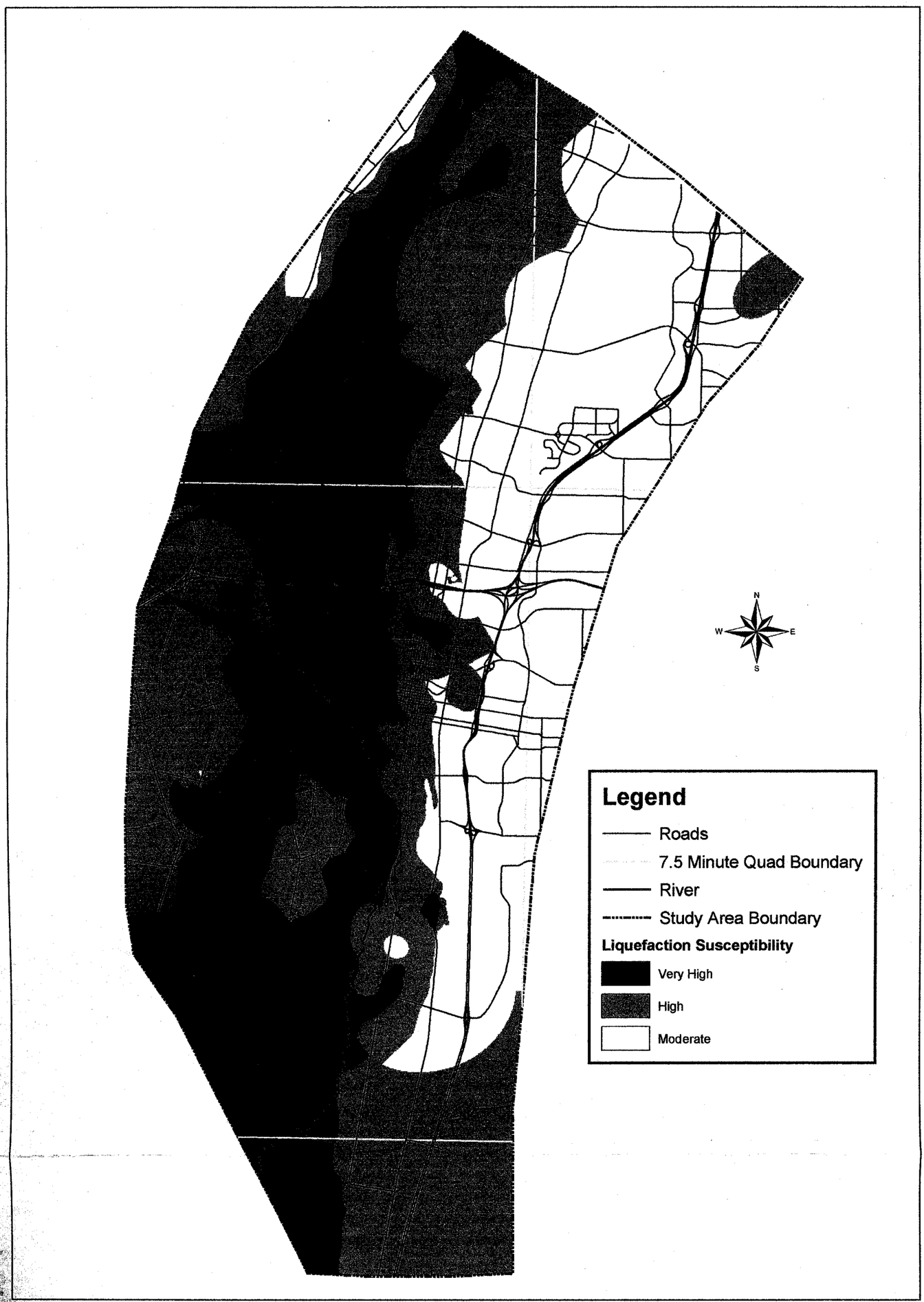

Figure 32. JAC Method B overall Worst Case Scenario Liquefaction Susceptibility Map.

CHAPTER 4. RESULTS

The JAC methods relied on shallow borehole data compiled for this study. The raw data from the driller's logs were expanded on where possible using ranges of values applicable to the soil types. However, the borehole data over the study area are sparse and clustered (Figure 14). On a regional to local scale there is also a high degree of spatial variability, although in some areas there are units that are laterally persistent (see Figures 15-18). These features make it difficult to interpolate data over the entire region; therefore JAC Methods A and B both have some artifacts of the interpolation scheme that can create uncertainty in the liquefaction susceptibility analyses. Figure 22 shows the reclassified grid for minimum percent fines for each of the three depth intervals. The "bull's-eyes" are artifacts of the interpolation process, indicative of high variability over a small distance. These artifacts tend to increase the uncertainty of the results in an analysis such as this, but can highlight areas where much more detailed analyses would be useful. Both JAC Methods A and B would exhibit less uncertainty for an area where the data were not sparse and clustered. For a site where data were more evenly spaced other geostatistical approaches such as kriging could be used as opposed to the ArcInfo *topogrid* command for the interpolation of data across the site.

Although the interpolation process does add a level of uncertainty to the JAC methods, the resulting liquefaction susceptibility maps exhibit the general regional trends one would expect to see in the study area. In this region where the soils in the study area

are dominated by sand and the water table meets the land surface along the river and slopes away to the east and west, one would expect to see a high correlation between the depth to water and the liquefaction susceptibility. Thus, the areas with the highest potential for liquefaction are along the river and in the flood plain with decreasing potential to the east and west, and virtually no potential for liquefaction outside the valley to the east and west where the elevation increases dramatically (Figure 1).

JAC Methods A and B were designed to evaluate liquefaction susceptibility not only at the ground surface, but also at depth, because soil units with a high or very high susceptibility to liquefaction at depth can cause problems such as subsidence of the ground surface. Figure 22 shows reclassified minimum percent fines for each depth interval. This particular parameter shows a decrease in percent fines or an increase in liquefaction susceptibility with depth, whereas the minimum SPT $(N_1)_{60}$ values (Figure 33) show an increase in the potential for liquefaction susceptibility in the 10-30 feet depth interval and a decrease in the 30-40 feet interval. The overriding issue is that there are obvious differences in these parameters with depth that control how the soil will react in the event of a major earthquake and that only taking into account the first few feet at the ground surface when evaluating a site for a critical facility such as a hospital or power plant could lead to disastrous consequences. There is some bias in the JAC methods results because there is more data available for the depth interval 0-10 feet than for the depth intervals 10-30 feet and 30-40 feet, as not all boreholes were completed to depths of 40 feet.

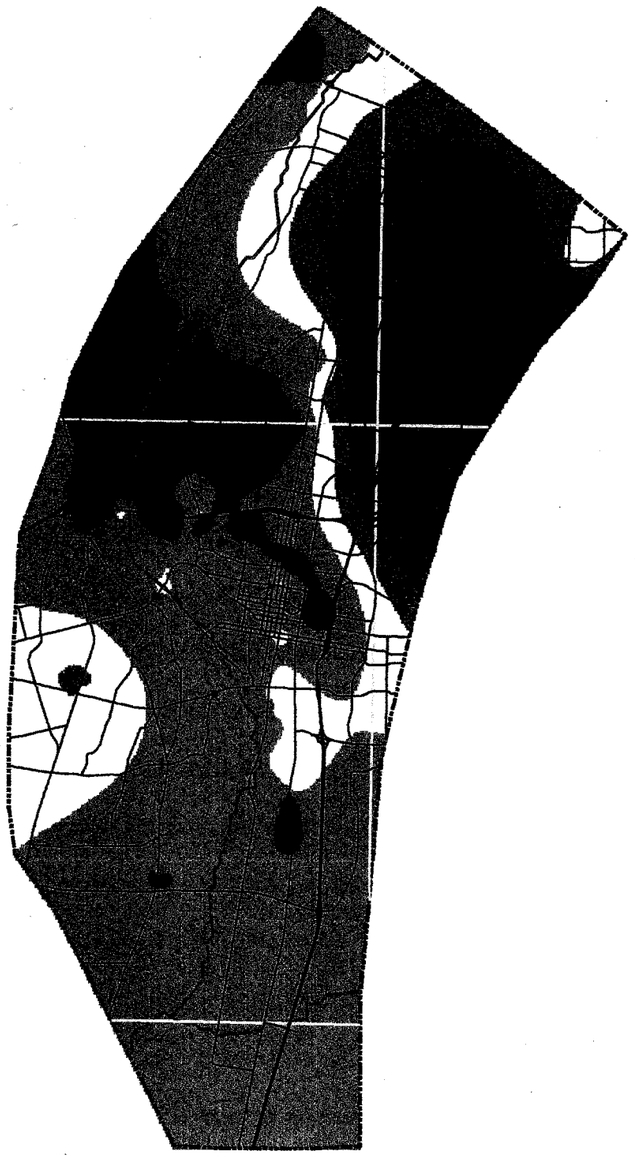

A.

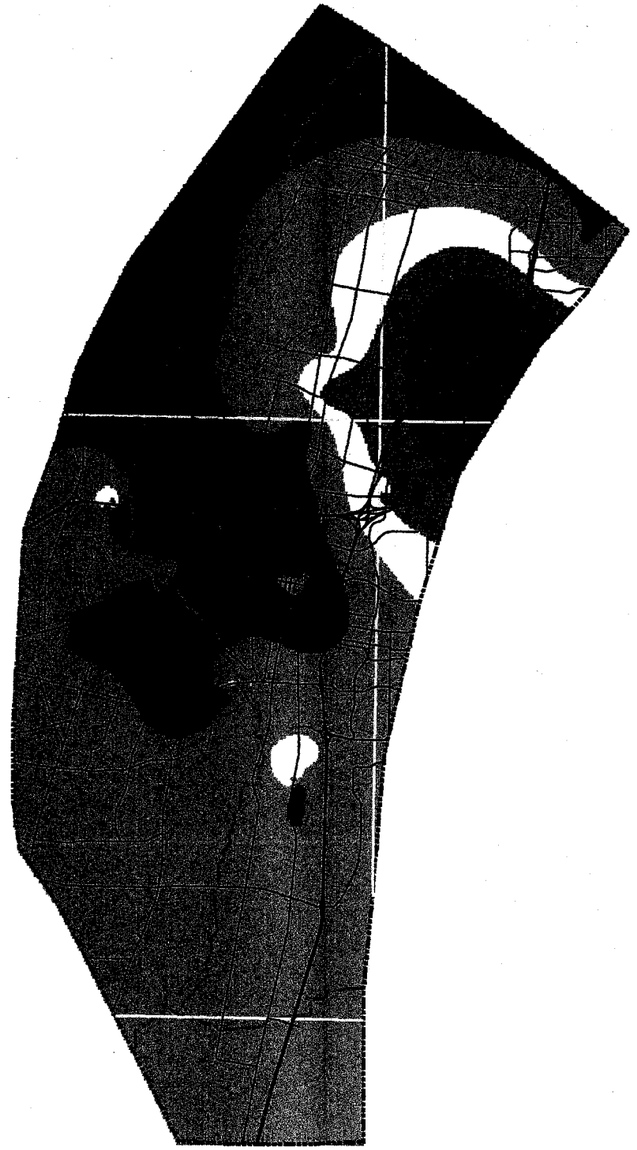

B.

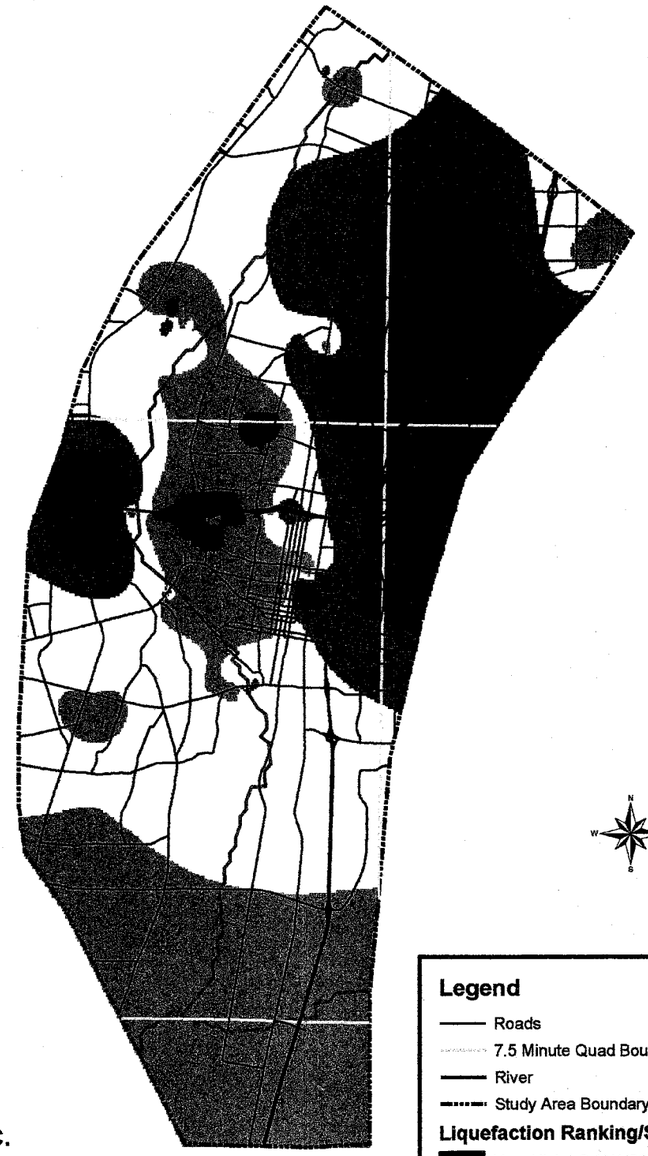

C.

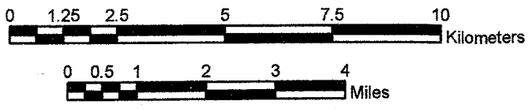

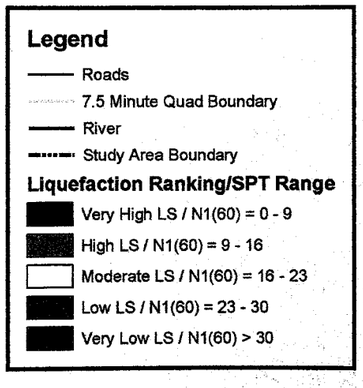

Figure 33. Reclassified maps of minimum SPT blow counts for three depth intervals A. 0 - 10 feet, B. 10 - 30 feet, and C. 30 - 40 feet.

CHAPTER 5. DISCUSSION

5.1 Comparison of JAC Methods A and B

JAC Methods A and B have been applied to the same study area for the same three depth intervals. JAC Method A is a more rigorous approach to evaluating liquefaction susceptibility. It incorporates the calculation of the Cyclic Stress Ratio (CSR) and a Peak Ground Acceleration (PGA) trigger based on the Seed Simplified Procedure (SSP), as discussed in Chapter 2. JAC Method B uses the normalized Standard Penetration Test (SPT) blow count ($(N_1)_{60}$) values as a proxy for the PGA trigger. JAC Method A was designed to evaluate whether or not this method could be used to minimize computation time and potentially allow for a simple means of evaluating liquefaction for a site in the field. The regional trends of the overall best and worst case liquefaction susceptibility results for JAC Method B (Figures 31-32) are similar to JAC Method A (Figures 29-30). However, JAC Method B exhibits a broader spread of values. There is a larger area of High liquefaction susceptibility in the worst case scenario and a larger area of Low liquefaction susceptibility in the best case scenario. JAC Method B seems to be a more conservative approach to evaluating the liquefaction susceptibility and JAC Method A, with its higher degree of detail, narrows the spread of values between the best and worse case scenarios. Thus, it appears that JAC Method B could be used as a fairly good proxy for evaluating the liquefaction

susceptibility for a quick broad overview of the liquefaction potential for a site, but the more rigorous JAC Method A should probably be used in evaluating sites where more detail is needed.

Additionally, uncertainty maps could be developed based on maps using several methods with varying or unknown reliabilities, such as those presented in this study. These uncertainty maps would show areas where all the maps produce the same level of liquefaction susceptibility as that level and all areas where the maps show different levels of liquefaction susceptibility as areas of uncertainty that would require additional evaluation. Unfortunately, uncertainty maps comparing the best and worst case of either JAC Method A or B would show almost 100% uncertainty. There are very small areas such as the center of the southern most part of the study area in Figures 29 and 30 where an uncertainty map between the best and worst-case scenarios would show consensus between the two scenarios. In this case both the best and worst case maps for JAC Method A show a moderate level of liquefaction susceptibility. However, should one create uncertainty maps to compare the best case results or the worst case results for the two methods (i.e. ccreate uncertainty maps from Figures 29 and 31 or 30 and 32), there would be a very small portion of the uncertainty map where the results are not consistent.

5.2 Comparison of JAC and WLA Methods

There is no way to evaluate the merits of one method for evaluating liquefaction susceptibility over another until there is actually an earthquake and occurrences of

liquefaction are mapped and compared to the various maps. Therefore, we must compare these methods theoretically and evaluate the pros and cons of each. We can also determine particular instances in which one method might be favored over another.

The WLA method provides a very smooth liquefaction map that is constrained by the surficial geology and depth to water. A surficial geology based method, even when borehole data are used to evaluate the liquefaction susceptibility of the various units, can mask potential hazards at depth especially in areas where there is a high degree of vertical variability, such as the Inner Valley of the Rio Grande. This type of approach is most suited to regions that do not exhibit very high variability in soil type with depth. The WLA method can also be used for evaluating the liquefaction susceptibility of a region where there is little available borehole data or where the borehole data are sparse or clustered, but good quality surficial geology maps exist, as was the case for this study area.

The JAC methods address some of the shortfalls of the WLA method, but introduce a level of uncertainty on the regional level. JAC Methods A and B take into account the spatial variability with depth that is masked by the surficial geology approach in the WLA method. Because of the sparse and clustered data that prompted WLA to use the method they did, there are artifacts and bias from the interpolation of data across the study area when presented on a regional scale. Additionally, the decrease in the number of data points with depth in the JAC analyses also introduces bias. However, JAC Methods A and B would likely prove to be more reliable for areas where data were more uniformly distributed. JAC Methods A or B should probably be used for sites where there are abundant borehole data that are not overly clustered, because these methods do

incorporate the potential for liquefaction at depth and provide a higher level of detail than the WLA method.

As discussed in the previous section the use of uncertainty maps could also be useful in comparing the results from these different methods. Uncertainty maps between the WLA method and JAC Methods A and B best-case scenarios would show a large amount of uncertainty in the central and western regions and more consistent results in the Very Low to Moderate liquefaction susceptibility levels to the east (Figues 12, 29, and 31), and uncertainty maps for the WLA and JAC Methods A and B worst case scenario show some areas of consistent results in the central portion of the study area along the river in the Very High to Moderate levels of liquefaction susceptibility and large areas of uncertainty to the east and west.

5.3 Implications and Caveats

The evaluation of liquefaction susceptibility is one facet of seismic hazard analysis. The primary goal of regional liquefaction analyses such as those presented in this study is to give a sense of the liquefaction susceptibility distribution and to provide for the delineation of areas where the potential for liquefaction hazard is most likely and should be evaluated in greater detail depending on the proposed use of a certain site or for locating critical facilities. The maps presented in this study should not be used for anything other than a suggestion of areas where there are obvious indications of a low potential for liquefaction or where a more comprehensive site-specific field investigation is needed.

If a more comprehensive field investigation were deemed necessary then it would be advisable to perform additional evaluations of liquefaction hazard on a smaller, more site-specific basis, using all available data and a more extensive method. The collection of additional data may also be necessary if gaps in the regional distribution of data appear in the area of interest.

Liquefaction susceptibility analyses and studies have become increasingly important to policy makers over the last several years as national initiatives by organizations such as the Federal Emergency Management Agency (FEMA) and National Earthquake Hazard Risk Priorities (NEHRP) have brought to the forefront the risks associated with earthquakes. The amount of damage and loss that continues to occur in places like Japan and California that have been preparing for and implementing earthquake preparedness policy and earthquake resistant structural building requirements for years has been a wake-up call to other locations where the potential for seismic activity exists. For liquefaction susceptibility maps to be useful for policy makers, it is necessary to look at the costs and benefits for the best and worst case scenarios. A best case scenario would be the most cost effective approach for policy makers in terms of hazard zonation for site analysis and requirements for building contractors, but the potential costs of damage and loss of life in the event of a major disaster would likely out-weigh those dramatically. However, hazard zonation or policy based on a worst case scenario would potentially be too cost prohibitive at the onset and would likely be too stringent as a workable solution. Liquefaction susceptibility study on a regional scale is not an exact science. Thus, it is generally a good idea for policy makers to be able to review both best and worse case liquefaction susceptibility scenarios as well as seismic

hazard probability maps so that decisions can be made on the basis of a range of potential hazards for specific types of site use. Critical structures such as hospitals and power plants should require more stringent guidelines than non-critical structures such as parking lots and playgrounds. Additionally, the use of uncertainty maps could be beneficial to policy makers when faced with the challenges of multiple sets of results. Unfortunately in the current study the range of values from the best and worst case scenarios of JAC Methods A and B are too broad to be helpful in terms of uncertainty because almost 100% of the study area would fall into the uncertain category. Augmentation of the existing database as new data becomes available and more stringent data screening would allow for more regional studies and uncertainty maps to be created that might be more beneficial to policy makers.

Evaluation of the results of each of these three methods in exact terms would require an earthquake and the subsequent mapping of liquefaction related ground failure. However, even this will not insure the delineation of the potential for liquefaction post-earthquake in the event of additional quakes. Studies of post-earthquake liquefaction distribution and comparison to prior liquefaction susceptibility maps in the San Francisco area have shown that there are few surprises as to the location of liquefaction since most areas where liquefaction occurred fit the criteria for liquefaction (CETS, 1994). However, there were broad areas mapped as susceptible to liquefaction where liquefaction did not occur. These differences can be caused by several factors that impact the liquefaction susceptibility mapping process as well: 1) the magnitude of the seismic event, 2) lower water tables than expected, and 3) local heterogeneity of deposits. Recurrence of liquefaction patterns was not uncommon either, in fact the distribution of

liquefaction caused by the 1989 Loma Prieta earthquake mimicked earlier liquefaction damage caused by the 1906 San Francisco earthquake, but the severity and damage were less in the more recent event. Areas where historic liquefaction has occurred are indicators of areas where liquefaction is possible, but past liquefaction events have the potential to change the characteristics of the soils, therefore they should be examined as well.

CHAPTER 6. CONCLUSIONS

Liquefaction related hazards can cause substantial damage to structures as well as loss of life in urban areas. Albuquerque is the largest urban area in New Mexico and is located within the most seismically active region of the Rio Grande rift. The Inner Valley of the Albuquerque Basin is underlain by unconsolidated, predominantly sandy alluvium; most of it is saturated with water. The water table meets the ground surface along the Rio Grande, then gently slopes away from the river (Thorn *et al.,* 1993). These conditions make Albuquerque a prime candidate for significant liquefaction related damage in the event of a large earthquake.

The liquefaction susceptibility maps presented in this study can provide a sense of the liquefaction susceptibility distribution and allow for the delineation of areas where the potential for liquefaction is high and should be evaluated in greater detail depending on the proposed use of a certain site or for locating critical facilities. There is no way to evaluate the accuracy of the three methods for liquefaction susceptibility presented in this study and be able to definitively say any one is better than another unless they are compared to the resultant liquefaction in the event of an earthquake. However, methods can be designed to address limitations or uncertainties not addressed by other methods with the goal of improving the reliability of the liquefaction maps for policy makers and earthquake preparedness and emergency management coordinators who need guidelines to work with before disaster strikes.

The WLA Method provides the best overall regional approach to evaluating liquefaction susceptibility for areas where good quality surficial geology maps exist, but there are limited data or where data are sparse and clustered. However, this method does exhibit a tendency to mask localized areas where the potential for liquefaction is much higher than the surficial geology indicates. If the available data for a region or a smaller localized site were more uniformly distributed then JAC Methods A or B would likely provide a more thorough analysis of liquefaction susceptibility because it takes into account sediment variation with depth and also brackets the results with best case – worst case scenarios. JAC Method A is generally most suited to sites where there is plenty of uniformly distributed data. It would also be the most rigorous method of those presented for specific site investigations where the potential for liquefaction has been suggested by regional studies such as the results presented herein for the Albuquerque area, and a highly detailed analysis is needed to determine the factor of safety for building on the site. JAC Method B is the most conservative method presented, and could be used to quickly do a field evaluation of a site to determine areas where a more rigorous approach such as JAC Method A might be needed.

All three methods presented show the same regional trend, in which the highest risk of liquefaction is along the river and floodplain. Liquefaction susceptibility decreases to the east and west as the elevation increases and the depth to groundwater increases. Each of the methods is best suited to particular uses, but none of them are without uncertainty or inherent error. Due to the high degree of spatial variability of the deposits in the Albuquerque area, the regional results presented in this study should only

be used to determine where a more thorough site investigation is necessary especially when locating residential, commercial and critical facilities.

The methods presented in this study are not site specific and could be applied to other locations. The limitation in these methods is in the constraints of the Seed Simplified Procedure, which provides a verified method for evaluating liquefaction hazard where sites are primarily "level to gently sloping terrain underlain by Holocene alluvial or fluvial sediment at shallow depths (less than 15 m (50 ft)" (NCEER, 1997). However, each of the methods presented here have different limitations and potential applications so the site and potential uses of the resulting liquefaction susceptibility maps should be evaluated and the best method for the particular characteristics and available data of the study area should be chosen.

References Cited

Bolt, B. A., 1993, Earthquakes: New York, W. H. Freeman and Company, 331 p.

CETS, 1994, Practical Lessons from the Loma Prieta Earthquake: Commission on Engineering and Technical Systems.

Connell, S. D., 1997, Geology of the Alameda 7.5-minute quadrangle, Bernalillo County, New Mexico: NMBG&MR, Open-File Digital Geologic Map 10, scale 1:24,000.

Connell, S. D., 2001, Stratigraphy of the Albuquerque Basin, Rio Grande Rift, Central New Mexico: A Progress Report: GSA Fieldtrip Guidebook, NMBG&MR Open File Report 454B.

Connell, S. D., Allen, B. D., Hawley, J. W., and Shroba, R., 1998, Geology of the Albuquerque West 7.5-minute quadrangle, Bernalillo County, New Mexico: NMBG&MR, Open-File Digital Geologic Map 17, scale 1:24,000.

Connell, S. D. and Love, D. W., 2001, Stratigraphy of Middle and Upper Pleistocene fluvial deposits of the Rio Grande (Post-Santa Fe Group) and the geomorphic development of the Rio Grande Valley, Northern Albuquerque Basin, Central New Mexico: GSA Fieldtrip Guidebook, NMBG&MR Open File Report 454B.

DMG, 1997, Guidelines for evaluating and mitigating seismic hazards in California: California Division of Mines and Geology, Special Publication 117.

dePolo, C. M., Rigby, J. G., Johnson, G. L., Jacobson, S. L., Anderson, J. G., and Wythes, T. J., 1996, Planning Scenario for a Major Earthquake in Western Nevada: Nevada Bureau of Mines and Geology, Special Publication 20, 128 p.

Deutsch, C. V. and Journel, A. G., 1998, GSLIB Geostatistical Software Library and User's Guide, 2nd Edition: New York, Oxford University Press, 369 p.

EQE, 1989,The October 17, 1989 Loma Prieta Earthquake, http://www.eqe.com/publications/lomaprie/lomaprie.htm

EQE, 1995, The January 17, 1995 Kobe Earthquake An EQE Summary Report, http://www.eqe.com/publications/kobe/kobe.htm

Hadj-Hamou, T., and Elton, D. J., 1989, A liquefaction susceptibility map for peninsular Charleston, South Carolina: Bulletin of the Association of Engineering Geologists, v. 26, n. 3, pp. 309-323.

Hawley, J. W., and Haase, C. S., 1992, Hydrogeologic Framework of the Northern Albuquerque Basin: New Mexico Bureau of Mines and Mineral Resources, OF-Report 387.

Hawley, J. W., Haase, C. S., and Lozinsky, 1995, An underground view of the Albuquerque Basin, In: Ortega-Klett, C. T. (ed), The Water Future of Albuquerque and Middle Rio Grande Basin: New Mexico Water Resources Research Institute, Technical Report No. 290, pp. 37-55.

Hawley, J. W., and Whitworth, T. M. (eds), 1996, Hydrogeology of potential recharge areas and hydrogeochemical modeling of proposed artificial-recharge methods in basin- and valley-fill aquifer systems, Albuquerque Basin, New Mexico: New Mexico Bureau of Mines and Mineral Resources, OF-Report 402-D.

Hwang, H., and Lin, H., 1997, Liquefaction susceptibility in Memphis and Shelby County, http://www.ceri.memphis.edu/~hwang/soil_lique/soil_lique.html

Idriss, I. M., 1997, Evaluation of liquefaction potential and consequences: Seismic Short Course on Evaluation and Mitigation of Earthquake Induced Liquefaction Hazards: NCEER Workshop, San Francisco, CA, March, 1997.

Kelley, V. P., 1977, Geology of Albuquerque Basin, New Mexico: New Mexico Bureau of Mines and Mineral Resources, Memoir 33, 59 p.

Kelson, K. I., Hitchcock, C. S., and Randolph, C. E., 1999, Liquefaction susceptibility in the Inner Rio Grande Valley near Albuquerque, New Mexico, Final Technical Report to USGS NEHRP.

Liao, S. S., and Whitman, R. V., 1986, Overburden correction factors for SPT in sand:Journal of Geotechnical Engineering, v. 112, n. 3, pp. 373-377.

Luna, R., 1993, Liquefaction analysis in a GIS environment, In: Frost, J. D. and Chameau, J. A. (eds),Geographic Information Systems and their Application in Geotechnical Earthquake Engineering: New York, American Society of Civil Engineers, pp. 65-71.

Mabey, M. A., 1997, Regional versus site specific spatial hazard analysis, In: Frost, J. D. (ed), Spatial Analysis in Soil Dynamics and Earthquake Engineering: New York, American Society of Civil Engineers, pp.29-41.

Macari, E. J., Martin, J. R., and Brandon, T. L., 1993, Liquefaction potential of Western Puerto Rico, In: Frost, J. D. and Chameau, J. A. (eds),Geographic Information Systems and their Application in Geotechnical Earthquake Engineering: New York, American Society of Civil Engineers, pp. 72-76.

Machette, M. N., 1998, Contrasts between short- and long-term records of seismicity in the Rio Grande rift – important implications for seismic hazard assessments in areas of slow extension *in* W. R. Lund (ed.) Western States Seismic Policy Council Proceedings Volume, Basin and Range Province Seismic Hazards Summit, Utah Geological Survey Miscellaneous Publication 98-2, p. 84-95.

Machette, M. N., Personius, S.F., Kelson, K. I., Haller, K. M., and Dart, R. L., 1998, Map and data for Quaternary faults and folds in New Mexico: US Geological Survey, OF-Report 98-521, 443 p.

Martin, J. R., 1993, Development of Geographical Information System (GIS) for seismic hazard study of Charleston, SC, In: Frost, J. D. and Chameau, J. A. (eds),Geographic Information Systems and their Application in Geotechnical Earthquake Engineering: New York, American Society of Civil Engineers, pp. 77-81.

National Center for Earthquake Engineering Research (NCEER), 1997, Summary Report of the 1996 Workshop on the Evaluation of Liquefaction Resistance of Soils.

National Research Council (NRC), 1985, Liquefaction of Soils During Earthquakes: National Academy Press, Washington, D. C.

Ohio EPA, 1996, Procedural and technical considerations for the seismic impact zones location restriction demonstration: DSIWM Guidance Document 0138, 14 p.

Ostadan, F., Arango, I., Litehiser, J., and Marrone, J., 1993, A prospect for liquefaction Hazard evaluation using GIS, In: Frost, J. D. and Chameau, J. A. (eds),Geographic Information Systems and their Application in Geotechnical Earthquake Engineering: New York, American Society of Civil Engineers, pp. 86-89.

Palmer, S. P., Walsh, T. J., Logan, R. L., and Gerstel, W. J., 1995, Liquefaction

Susceptibility for the Auburn and Poverty Bay 7.5-minute quadrangles, Washington: Washington Division of Geology and Earth Resources, Geologic Map GM-43.

Pannatier, Y., 1996, Variowin: software for spatial data analysis in 2D: New York, Springer, 91 p.

Personius, S. F., Machette, M. N., and Kelson, K. I., 1999, Quaternary faults in the Albuquerque area – an update: New Mexico Geological Society Guidebook, 50th Field Conference, Albuquerque Geology.

Poulos, S. J., Castro, G., and France, J. W., 1985, Liquefaction Evaluation Procedure: J. of Geotechnical Engineering, v. 111, n. 6, pp. 772-792.

Power, M. S. and Holzer, T. L., 1996, Liquefaction Maps: Applied Technology Council Tech Brief 1, 12 p.

Real, C. R., 1993, A geotechnically-oriented GIS for seismic hazard mapping, In: Frost, J. D. and Chameau, J. A. (eds), Geographic Information Systems and their Application in Geotechnical Earthquake Engineering: New York, American Society of Civil Engineers, pp. 90-94.

Robertson, G. P., 2000, GS+: Geostatistics for the Environmental Sciences. Gamma Design Software, Plainwell, Michigan USA.

Robertson, P. K., and Wride, C. E., 1997, Cyclic liquefaction and its evaluation based on SPT and CPT: Seismic Short Course on Evaluation and Mitigation of Earthquake Induced Liquefaction Hazards: NCEER Workshop, San Francisco, CA, March, 1997.

Sanford, A. R., Jaksha, L. H., and Cash, D. J., 1991, Seismicity of the Rio Grande Rift in New Mexico, In: Slemmons, D. B., Engdahl, E. R., Zoback, M. D., and Blackwell, D. D. (eds.), Neotectonics of North America, Geological Society of America Decade Map, v. 1, pp. 229-244.

Sanford, A. R., Olsen, K. H., Jaksha, L. H., 1981, Earthquakes in New Mexico: New Mexico Bureau of Mines and Mineral Resources, Circular 171, 20p.

Seed, H. B., 1979, Soil liquefaction and cyclic mobility evaluation for level ground during earthquakes: Journal of Geotechnical Engineering, v. 105, n. GT2, pp. 2-1-255.

Seed, H. B., De Alba, P., 1986, Use of SPT and CPT tests for evaluating the liquefaction resistance of sands, In: Clemence, S. P. (ed), Use of In Situ Tests in Geotechnical Engineering: New York, American Society of Civil Engineers, pp. 281-302.

Seed, H. B., and Idriss, I. M., 1971, Simplified procedure for evaluating soil liquefaction potential: Proceedings of the American Society of Civil Engineers, Journal of the Soil Mechanics and Foundations Division, v. 93, no. SM9, pp. 1249-1273.

Seed, H. B., and Idriss, I. M., 1982, Ground Motions and Soil Liquefaction During Earthquakes: Earthquake Engineering Research Institute Monograph.

Seed, H. B., Idriss, I. M., and Arango, I., 1983, Evaluation of liquefaction potential using field performance data: J. of Geotechnical Engineering, v. 109, n. 3, pp. 458-482.

Seed, H. B., Tokimatsu, K., Harder, L. F., and Chung, R. M., 1985, Influence of SPT procedures in soil liquefaction resistance evaluations: J. of Geotechnical Engineering, v. 111, n.12, pp. 1425-1445.

Seed, R. B., and Harder, L. F., 1990, SPT-based analysis of cyclic pore pressure generation and undrained residual strength, In: Duncan, M. J. (ed.), H. Bolton

Seed Memorial Symposium Proceedings, May, 1990: BiTech Publishers, Vancouver, B. C., Canada, pp.351-376.

Thorn, C. R., McAda, D. P., and Kernodle, J. M., 1993, Geohydrologic framework and hydrologic conditions in the Albuquerque Basin, central New Mexico: US Geological Survey, Water Resources Investigations Report, 93-9149, 106p.

Tosun, H., and Ulusay, R., 1997, Engineering geological characterization and evaluation of liquefaction susceptibility of foundation soils at a dam site, Southwest Turkey: Environmental and Engineering Geoscience, v. 3, n. 3, pp. 389-409.

UBC, 1994, Uniform Building Code.

Wong, I. *et al.,* 2000, Earthquake scenario and probabilistic ground shaking hazard maps for the Albuquerque-Belen-Santa Fe, New Mexico corridor: New Mexico Bureau of Mines and Mineral Resources.

Youd, T. L., 1973, Liquefaction, flow and associated ground failure, USGS Circular 688, 12 p.

Youd, T. L., 1975, Liquefaction, flow and associated ground failure: Proceedings of the Natl. Conf. On Earthquake Eng., Ann Arbor, Mich., June 18-20, 1975, pp. 146-155.

Youd, T. L., 1997, Updates on the simplified procedure: An overview of NCEER workshop in Salt Lake City on liquefaction resistance of soils: Seismic Short Course on Evaluation and Mitigation of Earthquake Induced Liquefaction Hazards: NCEER Workshop, San Francisco, CA, March, 1997.

Youd, T. L., 1998, Screening Guide for Rapid Assessment of Liquefaction Hazard at Highway Bridge Sites, Technical Report MCEER-98-0005, Multidisciplinary Center for Earthquake Engineering Research, Buffalo, New York.

Youd, T. L., 1999, Updating assessment procedures and developing a screening guide for liquefaction. In: Research Progress and Accmplishments 1997-1999, Multidisciplinary Center for Earthquake Engineering Research (MCEER), Buffalo, New York.

Youd, T. L. and Hoose, S. N., 1978, Historic ground failures in Northern California triggered by earthquakes, USGS Professional Paper 993, 177 p.

APPENDIX A

ARCINFO *topogrid* Command Background

The ARCINFO *topogrid* command is an interpolation method designed to generate hydrologically correct grids of elevation from point, line, and polygon coverages. It was based on the ANUDEM program developed by Michael Hutchinson (1988, 1989). For additional information about the ANUDEM program and its applications and examples see Hutchinson and Dowling (1991) and Hutchinson (1993). The method uses an iterative finite difference interpolation approach, that has been optimized to have the computational efficiency of methods such as inverse distance weighted interpolation, with the surface continuity of methods such as kriging and splines. Essentially, it is a discretized thin plate spline technique (Wahba, 1990). The iteration method uses a nested grid approach, which calculates the gridded data at successively finer resolutions. The process starts with a course grid spacing that is successively halved until the user defined grid spacing is reached. At each grid resolution the data points are allocated to the nearest grid point. Gauss-Seidel iteration with over-relaxation is used to determine values at grid points not occupied by data points. The Gauss-Seidel iteration matrix depends on a roughness penalty allows the fitted surface to follow abrupt changes in terrain, such as streams and ridges. It allows for abrupt changes in surface elevation, which is beneficial in the development of grids that are based on the irregularities of the natural ground surface and processes such as erosion and deposition. An over-relaxation parameter of 1.6 was empirically determined and found to accelerate convergence for the roughness penalties used (Hutchinson, 1989).

References

Hutchinson, M. F., 1988, Calculation of hydrologically sound digital elevation models. Third International Symposium on Spatial Data Handling, Sydney. Columbus, Ohio: International Geographic Union.

Hutchinson, M. F., 1989, A new procedure for gridding elevation and stream line data with automatic removal of spurious pits. Journal of Hydrology: 106, 211-232.

Hutchinson, M. F. and Dowling, T. I., 1991. A continental hydrological assessment of a new grid-based digital elevation model of Australia. Hydrological Processes: 5, 45-58.

Hutchinson, M. F., 1993, Development of a continent-wide DEM with applications to terrain and climate analysis, In: M. F. Goodchild et al (eds), Environmental Modeling with GIS. New York, Oxford University Press: 392-399.

Wahba, G., 1990, Spline models for observational data. CBMS-NSF Regional Conference Series in Applied Mathematics, Philadelphia: Soc. Ind. Appl. Maths.

This Thesis is accepted on behalf of the faculty
of the Institute by the following committee:

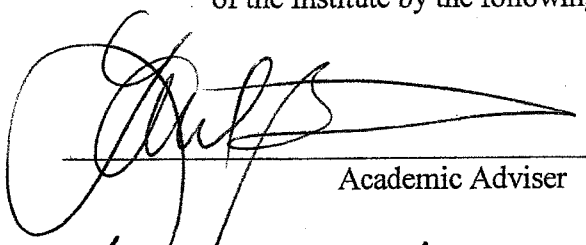

Academic Adviser

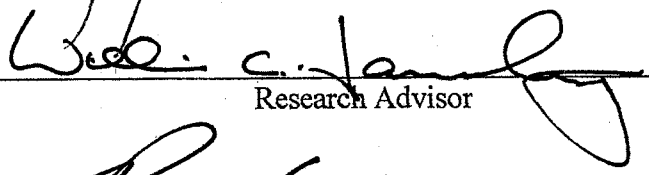

Research Advisor

Committee Member

Committee Member

Committee Member

January 12, 2004
Date

I release this document to New Mexico Institute of Mining and Technology

Jodi L. Clarke 18 January 2004

Students Signature Date